Journal of Asian Earth Sciences 40 (2011) 52–71

Contents lists available at ScienceDirect

Journal of Asian Earth Sciences

journal homepage: www.elsevier.com/locate/jseaes

Sedimentology of early Pliocene sandstones in the south-western Taiwan foreland: Implications for basin physiography in the early stages of collision

Sébastien Castelltort [a,*], Stefan Nagel [a], Frédéric Mouthereau [b,c], Andrew Tien-Shun Lin [d], Andreas Wetzel [e], Boris Kaus [a], Sean Willett [a], Shao-Ping Chiang [d], Wei-Yi Chiu [d]

[a] Department of Earth Sciences, ETH Zürich, Sonneggstrasse 5, 8092 Zürich, Switzerland
[b] UPMC Univ Paris 06, UMR 7193, Institut des Sciences de la Terre de Paris, F-75005 Paris, France
[c] CNRS, UMR 7193, Institut des Sciences de la Terre de Paris, F-75005 Paris, France
[d] Department of Earth Sciences, National Central University, 300 Jungda Road, Chungli, Taoyuan, Taiwan
[e] Geological – Paleontological Institute, University of Basel, Bernoullistrasse 32, 4056 Basel, Switzerland

ARTICLE INFO

Article history:
Received 18 January 2010
Received in revised form 24 August 2010
Accepted 6 September 2010

Keywords:
Foreland basin
Pliocene
Taiwan
Collision
Monsoon
Turbidites
Tidal rhythmites

ABSTRACT

This work presents sedimentological observations and interpretations on three detailed sections of the Pliocene Yutengping/Ailiaochiao formations, deposited in the early stages of collision in Taiwan. Seven facies associations record paleoenvironments of deposition ranging from nearshore to lower offshore with a strong influence of tidal reworking, even in shelfal sub-tidal environments, and a pro-delta setting characterized by mass-flows. The association of shallow facies of the upper offshore to lower shoreface with pro-delta turbidite facies sourced in the orogen to the east suggests a peculiar setting in which turbidite deposition occurred below wave base but on the shelf, in water depths of probably less than 100 m. This adds to the examples of "shallow turbidites" increasingly commonly found in foreland basins and challenges the classical view of a "deep" early underfilled foreland basin. Time series analysis on tidal rhythmites allow us to identify a yearly signal in the form of periodic changes of sand-supply, energy and bioturbation that suggests a marked seasonality possibly affecting precipitation and sediment delivery as well as temperature. The Taiwan foreland basin may also present a potentially high-resolution record in shallow sediments of the early installation of monsoonal circulation patterns in east Asia. We confirm partly the paleogeography during the early stages of collision in Taiwan: the Chinese margin displayed a pronounced non-cylindrical geometry with a large basement promontory to the west in place of the modern Taiwan mountain range. Collision in Taiwan may have happened at once along the whole length of the modern mountain range, instead of progressively from north to south as classically considered.

1. Introduction

Foreland basin sediments preserve a unique record of the tectonic and climatic processes that construct and destroy topography during plate collision (Allen et al., 1986). As such their study is fundamental for the understanding of mountain building processes. The foreland basin situated to the west of the Taiwan mountain ranges is of particular interest because it contains a record of the evolution of one of the best known and most studied orogens.

The island of Taiwan is situated on the boundary between the Philippine Sea Plate and the Eurasian Plate and is a textbook example of an arc-continent collision (Ho, 1986; Sibuet and Hsu, 1997; Suppe, 1984). Subduction of the South China Sea as part of the Eurasian Plate (EUR) beneath the Luzon Arc on the Philippine Sea Plate (PSP) has progressively consumed the oceanic crust and the Luzon Arc is presently colliding with the passive margin of Eurasia creating the mountain belt of Taiwan since the Late Miocene (Fig. 1). The obliquity between the passive margin and the Luzon Arc seems to result in a "zippering" effect of progressive closure of the South China Sea towards the south, such that the collision would be older in northern Taiwan than in southern Taiwan. Furthermore, the high rates of convergence (Seno et al., 1993; Yu et al., 1997), high rate of rock uplift and the wet, stormy climate of the sub-tropical typhoon belt combine to produce erosion and sediment yield rates amongst the highest in the world (Dadson et al., 2003). These characteristics make Taiwan one of the world's foremost natural laboratories to study orogenesis and foreland basin development.

The progressive arc-continent collision and its southward propagation has been extensively studied, numerous tectonic studies and models address the collisional process (Barr and Dahlen, 1989; Chemenda et al., 2001; Dahlen and Barr, 1989; Ernst and

* Corresponding author. Tel.: +41 44 632 36 48; fax: +41 44 632 14 22.
E-mail address: sebastien.castelltort@erdw.ethz.ch (S. Castelltort).

1367-9120/$ - see front matter © 2010 Elsevier Ltd. All rights reserved.
doi:10.1016/j.jseaes.2010.09.005

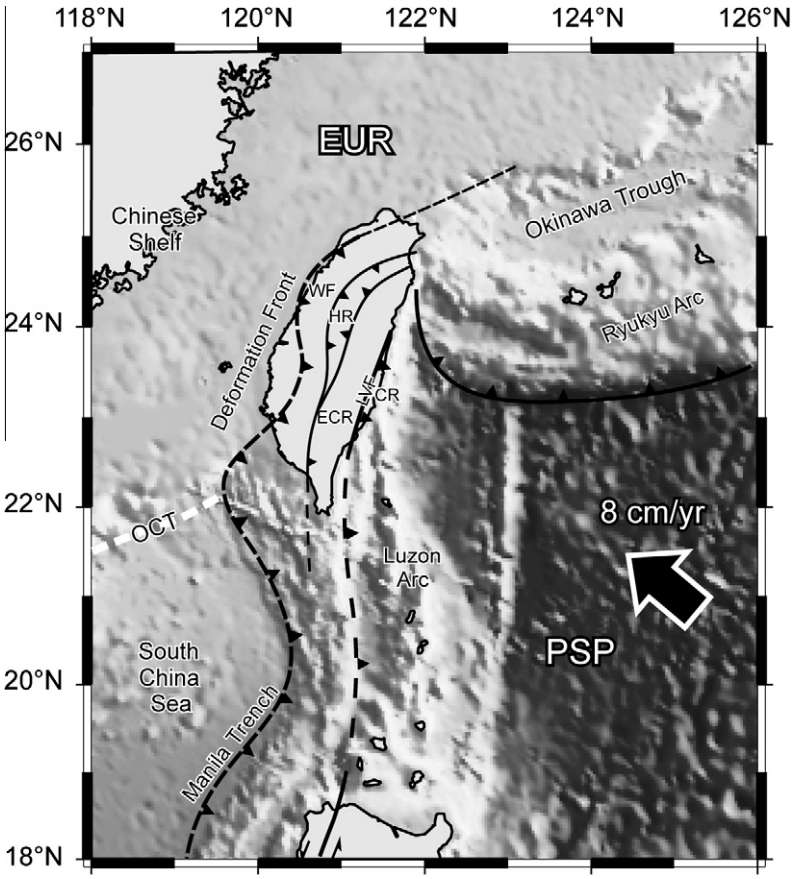

Fig. 1. Geodynamic context of the collision in Taiwan. PSP: Philippine Sea Plate; EUR: Eurasian Plate; WF: western Foothills; HR: Hsüehshan Range; ECR: Eastern Central Range; LVF: Longitudinal Valley Fault; CR: Coastal Range; OCT: Ocean–Continent Transition.

Jahn, 1987; Fuller et al., 2006; Liu et al., 2001; Suppe, 1981, 1984; Wu et al., 1997). The development of the foreland basin as a loading and sedimentation response to the mountain building has also been largely documented (Chen et al., 2001a; Chiang et al., 2004; Covey, 1986; Lin and Watts, 2002; Lin et al., 2003; Simoes and Avouac, 2006; Teng, 1991; Tensi et al., 2006).

However, despite the extensive amount of work done there exists as yet no comprehensive synthesis of the syn-orogenic depositional environments and the associated paleogeography of the basin, and of the sediment transport systems originating in the orogen. It is essential to fill this gap in knowledge in order to derive detailed analysis of the spatio-temporal evolution of the subsidence and sedimentary fill and its relationship to tectonic and denudational events in the orogenic belt. It is a long-term objective to re-evaluate Taiwan's collisional paleogeography in the light of new data in order to render tectonic and geomorphic reconstitutions possible. The present paper represents a first analysis of three sections measured in detail in south-western Taiwan that provide information on the early Pliocene paleogeography and dynamics of the sedimentary system at the beginning of the collision.

The foreland basin of Taiwan is one of the first basins where a "foreland sequence" with a underfilled to overfilled transition was identified (Covey, 1986). By studying the Plio-Pleistocene deposits of the western Taiwan foreland basin from north to south, Covey (1986) proposed an evolutionary model of a foreland basin in relation with the growth stage of the adjacent orogen comprising an initial transgressive stage at the initation of foreland basin subsidence, a deep water stage when subsidence exceeded sediment input from the growing orogen, and a third steady-state shallow water to fluvial stage when the foredeep was at steady state and sediment supply by-pass the plain to outer deeper environments. This model was influenced by (1) the emerging paradigm of Taiwan's southward propagation (Suppe, 1981), and (2) the observation of the current sub-marine setting south of Taiwan where deep sea fans actively form on the continental slope to basin settings in front of the accretionary wedge. It is crucial for the paleogeography of Taiwan to search for indications of paleo-water depth in the early stages of the collision in order to better understand the tectonic setting at that time. This has important implications for the general understanding of foreland basin development.

The objective of this paper is to present a detailed analysis of the facies encountered in the studied sections and their interpretation in terms of paleoenvironments in the Western Foreland Basin. We then discuss the physiographic implications for the early stages of collision.

2. Geological setting

2.1. The Taiwan orogen

The Taiwan orogen developed on the Chinese continental margin in response to the convergence between the EUR and the PSP (Ho, 1986; Suppe, 1980). The convergence velocity of the PSP relative to the EUR plate is of the order of 7–8 cm y^{-1} (Seno et al., 1993; Yu et al., 1997). The general structure of the range is composed of several units (Fig. 1). To the east, the "Coastal Range" (CR) represents the part of the Luzon Arc that is presently colliding with the Chinese continental margin. It is constituted by Miocene volcanic rocks and intra-arc flysch basins. The suture zone separating the CR from the Chinese continental margin is represented by the "Longitudinal Valley" (LV), a narrow depression underlain by

one or more major active faults (e.g. the Longitudinal Valley Fault, Tsai, 1986). The LV is bounded to the west by the "Eastern Central Range" (ECR) where the Mesozoic basement of the Chinese margin outcrops up to 2000 m above sea level. To the west, the Hsüehshan Range (HR) is composed of Paleogene sediments having experienced low grade metamorphism interpreted as a Paleogene trough (Teng, 1996) inverted during the Neogene. Further to the west are the "western Foothills" (WF), a typical foreland fold-and-thrust belt made of west-vergent thrusted Neogene clastic sedimentary units (Fig. 2). The "Coastal Plain" is the youngest terrestrial unit, and represents the onland continuation of the adjacent current marine foreland trough of the Taiwan Strait.

2.2. The Western Foreland Basin

In Taiwan, the Western Foreland Basin (WFB) results from the flexure of the EUR lithosphere provoked by thrust loading of units onto the Chinese margin. Field work, seismic profiles and borehole data acquired by oil companies document extensively the development of the basin. It can be subdivided into two distinct units: a foreland fold-and-thrust belt buried by synorogenic sedimentation, the WF or "wedge-top" depozone, and a frontal trough or "foredeep" lacking major structures which encompasses the Coastal Plain and extends further into the current Taiwan Strait to the west (Fig. 2).

Seismic profiles and borehole geophysical data (Taiwan, CPC Corporation) have permitted the identification of a major unconformity at the base of syn-collision series in the WFB (Lin et al., 2003; Tensi et al., 2006; Yu and Chou, 2001). Using four cross-sections along the basin, Yu and Chou (2001) have shown that the stratigraphic hiatus increases over a distance of 50 km from the current frontal thrust to what they identify as the current forebulge. In the Taihsi basin, offshore in the Taiwan Strait, this unconformity marks the boundary between the Nanchuang formation below (supposedly pre-collision) and the Kueichulin formation above (syn-collision). This boundary has been estimated to have formed at 6.5 Ma (Lin et al., 2003) thanks to the 7.6–7.1 Ma K-Ar age of a basaltic layer ~25 m below the unconformity (Juang, 1996), and the presence of nannofossils giving 8.6/5.6 Ma at the base of the Kueichulin formation (Lin et al., 2003). Onshore, 40–50 km east of the Taihsi basin, in the fold-belt of the WF, field data indicate an Upper Miocene age for the same boundary (e.g. Ho, 1988) which has long been interpreted to mark the change from pre- to syn-collisional series. A slightly older age of ~8.6 Ma from biostratigraphic data is found further eastward which is perhaps consistent considering that the flexure may have propagated from east to west with the migration of the load (Tensi et al., 2006). The age of the first syn-collisional sediments is thus not yet well constrained.

As a whole the evolution of syn-collision facies seems to be similar from north to south, as described initially by Covey (1984, 1986). The general sequence comprises first a retrogradational succession of the Kueichulin and the Chinshui Shale Shale formations, followed by a progradational succession of the Cholan and Toukoshan formations (Fig. 3).

This paper focuses on the upper Kueichulin formation, i.e. early-middle Pliocene.

The Kueichulin formation is transgressive over the basal foreland unconformity. It is constituted essentially by siliciclastics of a shallow marine deltaic environments often dominated by the influence of tides. The sea level rise associated to this formation marks the onset of load induced subsidence by the growing orogen. To the south, the Kueichulin formation progressively passes to deposits of the turbiditic Gutingkeng formation (also coeval with the subsequent Chinshui Shale and Cholan formations, cf. Fig. 3). These are thought to represent deeper marine environments of upper continental slope to outer shelf environments, but their association with reefal formations (Gong et al., 1998) casts questions about their actual precise depositional depth. The Kueichulin formation reaches a thickness of 800 m at its main depocentre east of the Hsinchu–Taoyuan area. The source of sediments during the Kueichulin deposition is thought to be essentially the same as during the previous passive margin history of the basin, i.e. from the Eurasian continent to the west, and also from the north-east of the emerging Taiwan orogen (Shaw, 1996). This, however, remains a matter of further investigations.

The middle-late Pliocene Chinshui Shale formation is around 100–200 m thick and reaches more than 300 m at its depocentre. It is mostly represented by fine-grained detrital sediments (silts and shales). Reworked fossils and paleocurrent directions indicate that the main source of the basin fill at this period was the Taiwan orogen to the east (Covey, 1986).

The upper Pliocene and lower Pleistocene Cholan formation represents a marine-continental transition with tidal influence which becomes progressively dominated by fluvial processes upwards. Typically it consists of fine grey/brown sediments alternating with fine to coarse sands. It reaches 1500 m in thickness and has an overall wedge-shaped geometry thinning westward and being more elongate along strike than the two preceding formations which probably is related to an increased influence of the frontal structures and to the acquisition of a larger-scale geometry of the range. The source of the sediments at this time is clearly the Taiwan range to the east (Ho, 1988).

The buildup of the range then accelerates during deposition of the Toukoshan formation and its equivalent which reaches up to 3000 m in thickness. It is mainly made of coarse alluvial sediments which probably correspond to sands and conglomerates deposited in braided rivers and alluvial systems *s.l.* (Covey, 1984, 1986).

The spatio-temporal history of the WFB is interpreted as an evolution from an "under-filled" stage with marine depositional environments deepening upwards and relatively low sedimentation rates (Kueichulin formation and lower Chinshui Shale formation) towards an "over-filled" stage marked by the filling of the basin with deposits formed in progressively shallower environments upwards and eventually becoming continental (Cholan and Toukoshan formations, Covey, 1984, 1986).

The WFB series onshore and offshore are very well dated thanks to nannoplankton and foraminifer studies calibrated with magnetostratigraphy (Chang and Chi, 1983; Horng and Shea, 1996; Huang, 1984) and the more recent work of Chen et al. (2001a).

3. Sedimentological observations in the Yutengping Sandstone and Ailiaochiao formations

During the course of this study three sections have been measured and described in detail. They are localised in the Jioucyongping syncline of the Meishan area (section A, Figs. 2–4), in the Yuching syncline on the Tseng Wen River close to the toll station (section B, Figs. 2, 3 and 5) and close to the dam upstream (section C, Figs. 2, 3 and 6).

These sections preserve paleoenvironments in the late Kueichulin formation (retrogradational stage of the underfilled foreland). In the Meishan area, section (A) is situated in the "Tawo" group of siltstones and sandstones (Chang, 1955; Lin et al., 2004), equivalent to the broader formation of the "Yutengping Sandstone" which corresponds to the last stage of the Kueichulin formation (Ho, 1988; Lin, 1954). In the Yuching syncline, the sections (B) and (C) are situated in the Ailiaochiao formation (Chen et al., 2000; Lin et al., 2005) which also corresponds to the Yutengping Sandstone (Ho, 1988). Both the Yutengping Sandstone and

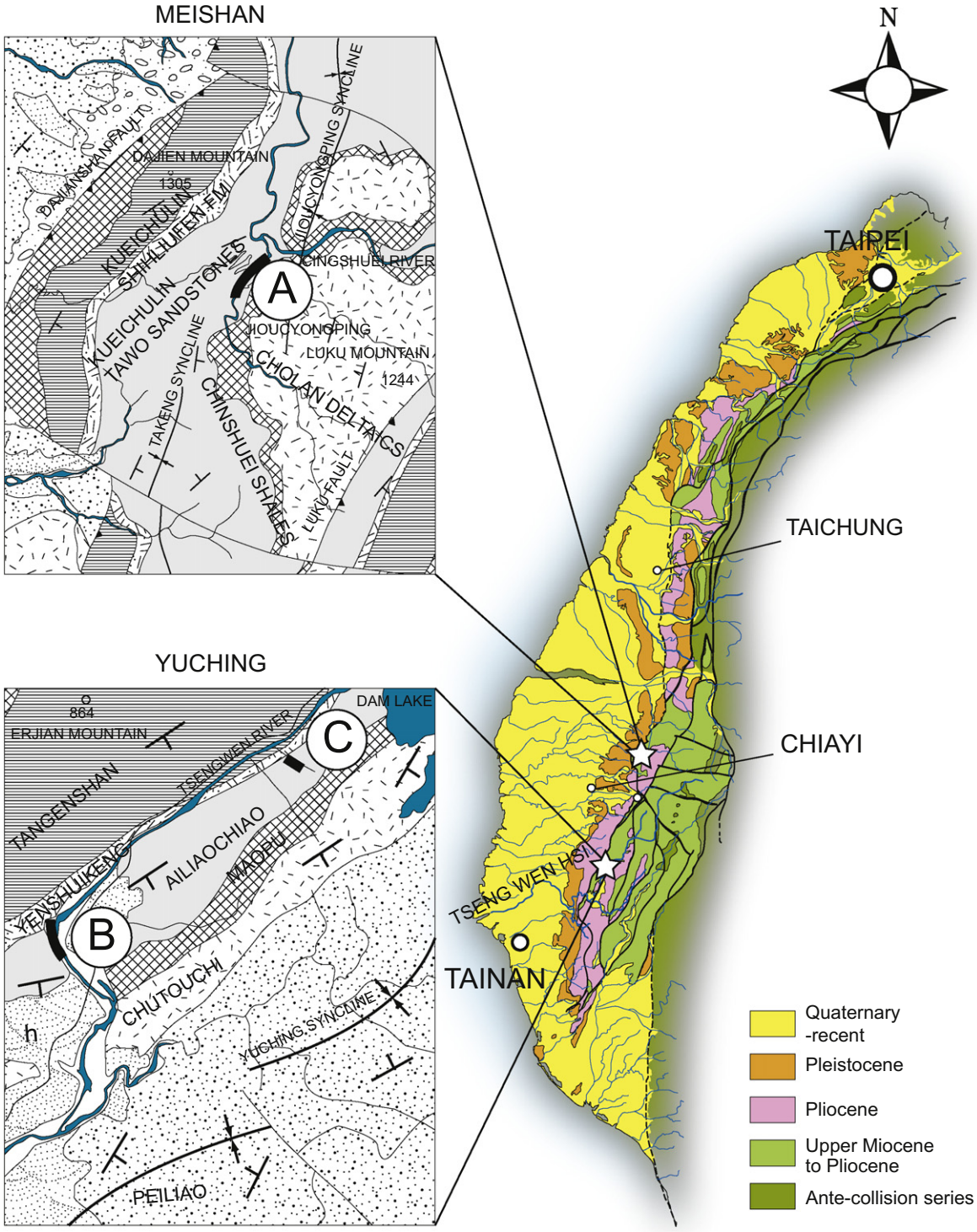

Fig. 2. Location map of the sections studied in this work. (A) "Meishan" section; (B) "Tseng Wen Toll" section; (C) "Tseng Wen Dam" section. The color map to the right shows the fold-and-thrust structure of the western Foothills and the recent fluvial deposition in the coastal plain. The sections are situated in the external synclines of the belt. Maps have been redrawn from the geological maps Sinhua and Yunlin (Lin et al., 2005, 2004). The names of the formations are marked for reference but the reader is referred to original maps for legends.

Ailiaochiao formations are known to represent shallow-water depositional environments (Ho, 1988).

The general characteristics of the observed sediments confirm a shallow-water depositional environment and point to the dominant role of tides and supply events from the feeding river systems in the form of mass flows deposited in shallow water.

3.1. Facies association 1: clays and siltstones (Fig. 7, occurrence: Meishan, TsengWen Toll & dam)

3.1.1. Description

These facies are constituted of mixed, poorly sorted, clay to silt sediments forming dark intervals of lower relief than the

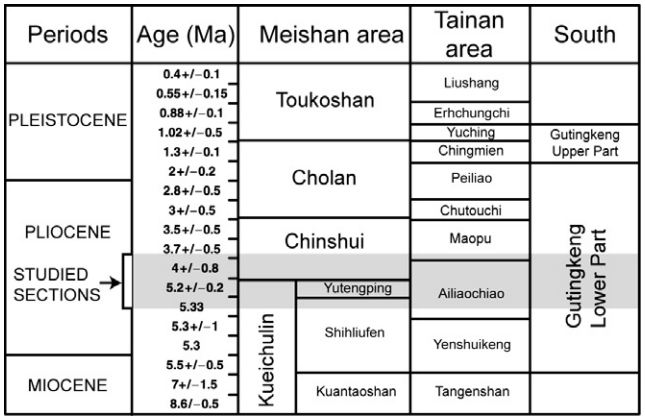

Fig. 3. Stratigraphic context and formation names. The studied sections are situated in the late Kueichulin formation subgroups of Yutengping Sandstone and Ailiaochiao, deposited in the early stage of collision. The early Kueichulin formation corresponds to the transgressive stage of the foreland basin. The late Kueichulin formation, Chinshui Shale formation and lateral equivalents correspond to the "under-filled" stage of the foreland basin". The Cholan formation and Toukoshan formation represent the filling and over-filling of the basin (Covey, 1986). Numeric ages refer to the lower mark of each interval.

surrounding sandstone beds. Their thickness ranges from several centimetres to several decimetres. They contain little to no bioclastic material and no observable bioturbational structures.

3.1.2. Interpretation

These fine-grained sediments are most probably deposited by low velocity currents and/or suspension fall-out at the end of more energetic event flows. The near absence of remains of organisms suggests a dominantly clastic origin of the supply process, perhaps tidal, riverine or combined in origin. It precludes an origin by solely reworking of shallower environments like storms. The absence of burrows suggests a relatively high rate of deposition. They can be found in all offshore associations associated with tidal and turbiditic environments.

3.2. Facies association 2: bioturbated clays and siltstones (Fig. 7, occurrence: Meishan)

3.2.1. Description

These facies comprise dark grey structureless intervals of clays and silts of several decimetres to several metres of thickness (Fig. 7 A). They contain a relatively high concentration of foraminifera and clasts of bivalves, echinoids and gastropods. Bioturbation has been sometimes intense and has totally churned the sediment. Some burrows are marked by shell concentrations but due to the soft nature of the sediment they are generally difficult to identify while mainly being biodeformational structures. Most of them could be ascribed to the branching networks of *Thalassinoides*.

3.2.2. Interpretation

The depositional environment of this facies association is similar to FA1 but with a lower sedimentation rate that allows for colonization by organisms and subsequent bioturbation. The higher content in bioclasts and the large thickness also suggest a relatively stable environment of continuous low rate of suspension settling and occasional silt input.

3.3. Facies association 3: completely bioturbated silts and sands (Fig. 7, occurrence: Meishan and TsengWen Toll)

3.3.1. Description

Tabular beds of greyish siltstone (FA3.1) and sandstone (FA3.2) of several decimetres thickness having generally planar and non-erosive bed boundaries that have been intensely bioturbated. Generally, burrows overprint the primary sedimentary structures, but in rare cases either parallel fine lamination, or small-scale wavy bedding with current ripples, or scour-and-fill structures and possible small-scale (dm) hummocky cross-stratification can be observed (Fig. 7 B).

This facies displays the highest diversity of trace fossils (Fig. 7C and D). The burrows are ascribed to the ichnogenera *Ophiomorpha*, *Thalassinoides*, *Schaubcylindrichnus*, *Cylindrichnus*, *Chondrites*, *Asterosoma*, *Siphonichnus*, *Phycosiphon*, *Planolites*, *Conichnus* and *Teichichnus*. The dominating traces are vertical, horizontal, inclined, sinuous and branching networks of *Ophiomorpha* and *Thalassinoides*. Very abundant too are burrows of *Schaubcylindrichnus* marked by whitish walls, and forming isolated, vertical, inclined and large concave-up U-shaped burrows.

These facies contain also numerous centimetric pieces of organic material (wood, leaves debris) floating in the sandstones that can be found relatively well preserved or as stained rusty spots on the rock.

3.3.2. Interpretation

The encountered trace fossils are characteristic of the distal *Cruziana* ichnofacies, indicating lower offshore depositional environments according to existing trace fossil models in shallow marine systems (Pemberton et al., 2001). The style of the bioturbation is in good agreement with the fine-grained lithology and the rare physical structures observed. The intense reworking of sediments by organisms and the fine grain size suggest distal input of clastics in a stable environment with relatively low, mainly continuous sedimentation rate.

3.4. Facies association 4: Teichichnus dominated heterolithics of laminated silts and sands (Figs. 7 and 8, occurrence: Meishan and TsengWen Toll)

3.4.1. Description

This association comprises laminated siltstones and sandstones characterized by dominant *Teichichnus* burrows (FA4.1) and non-bioturbated laminated siltstones and sandstones (FA4.2).

The bioturbated beds (FA4.1) are decimetric to pluridecimetric beds of yellow, violet to grey coloured siltstones and sandstones (Fig. 7 E). Their internal structure is made-up by generally banded, wavy, mm-to-cm thick siltstone to very fine sandstone layers and small current ripples alternating with millimetric clayey–silty lamination. This bedding is disrupted by various burrows among which slightly concave-upward arcuate retrusive forms of *Teichichnus rectus* sometimes almost completely dominate (Fig. 7 F). Other, less abundant trace fossils include *Ophiomorpha*, *Thalassinoides*, *Tasselia*, *Bergaueria*, *Conichnus*, *Taenidium*, *Siphonichnus* and *Paleophycus*. This form of *Teichichnus* could be mistaken for *Diplocraterion parallelum* var. *quadrum*, a specific variety of *D. parallelum* (Fürsich, 1974) described as prominent in the distal embayment facies (Ekdale and Lewis, 1991).

The non-bioturbated beds (FA4.2) are characterized by thin clayey–silty lamination alternating with silt-to-sand layers in variable proportion, producing mainly parallel laminated, very fine, well sorted sandstones, or wavy and lenticular small-scale (cm) heterolithics with ripples and micro cross-lamination (Fig. 8 A). The ripples are dominated by very small ($\leqslant$1 cm of amplitude) asymmetric forms often showing bi-directional flow azimuths.

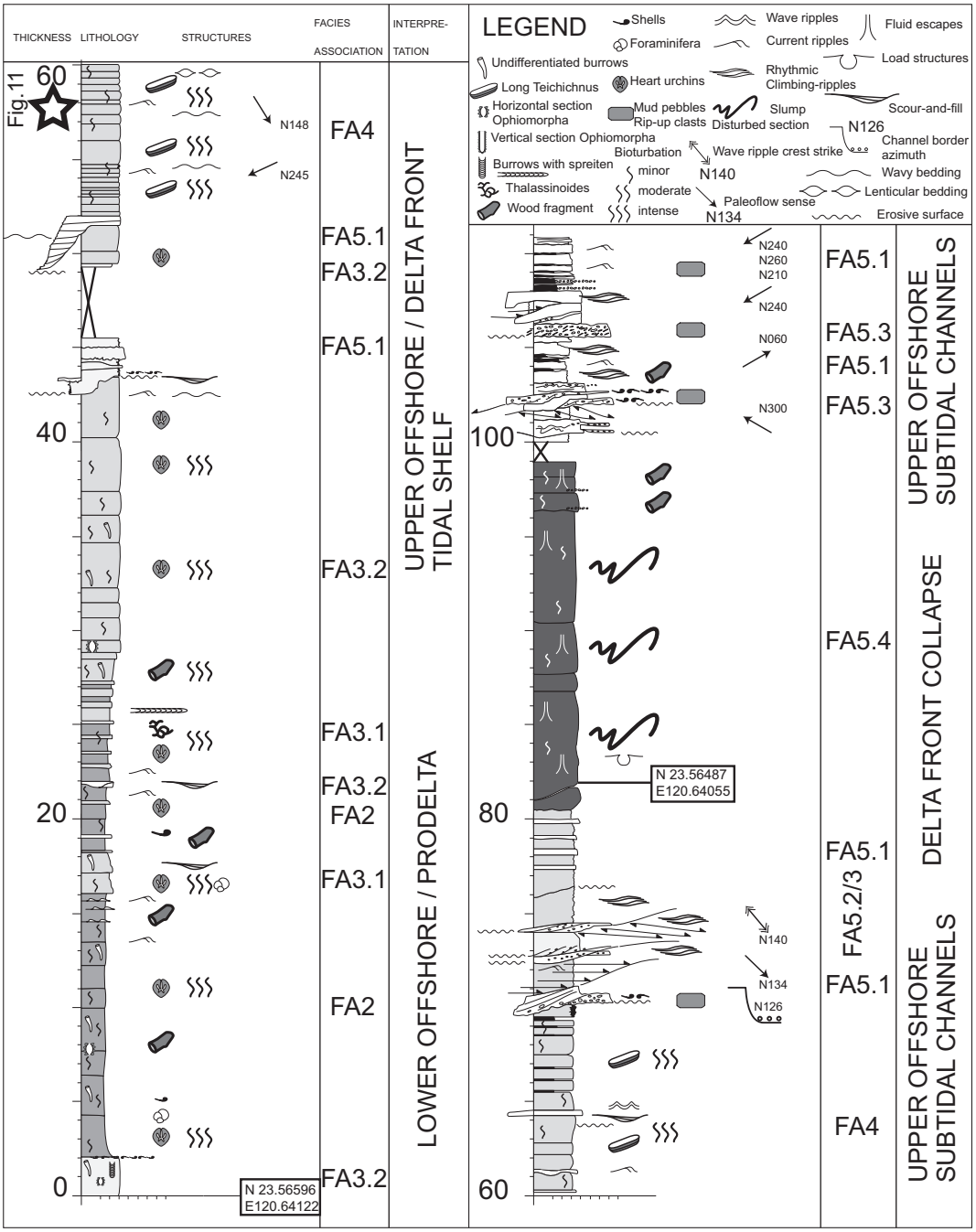

Fig. 4. Meishan, section (A), synthetic stratigraphic column (see Fig. 2 for location). Note location of the Fig. 11 (star at 57 m).

Large forms are also present, and bundled, more symmetrical forms of possible wave origin can be found.

3.4.2. Interpretation

The fine-laminated character of these facies documents alternating periods of currents with periods of quiet settling of the finer particles, the bidirectional azimuths indicated by current ripples and the occurrence of wave ripples all suggest a shallow marine tidal origin for the FA4. Even though in many places, one current direction appears to dominate, the occurrence of bipolar flow directions always covered with fine-grained material implies deposition in sub-tidal environments. The spectral analysis of wavy rhythmites of the FA5 underneath confirms the tidal character. The overwhelming dominance of *Teichichnus* bioturbation points to stressed conditions normally typical of marginal-marine successions. Commonly, monospecific assemblages of short *Teichichnus* are restricted to inter-distributary bays (Pemberton et al., 2001), the encountered elongate *Teichichnus*, however, could point to more open marine conditions (Pemberton et al., 2001). Carmona et al. (2009) suggested, for very similar setting in lower Miocene deposits in Patagonia, deposition in a pro-delta environment where freshwater influx alternates with periods of normal-marine salinity conditions (Buatois et al., 2008). The ichnofauna being more diverse than in restricted environments and the association with the burrows of the open-marine suite support more open marine conditions.

By analogy with the current setting in the Taiwan Strait (Boggs, 1974) and in the Yellow Sea/east China Sea (Johnson and Baldwin, 1996), these facies appear to correspond to offshore muddy sediments deposited in sub-tidal settings on the shelf, in the distal parts

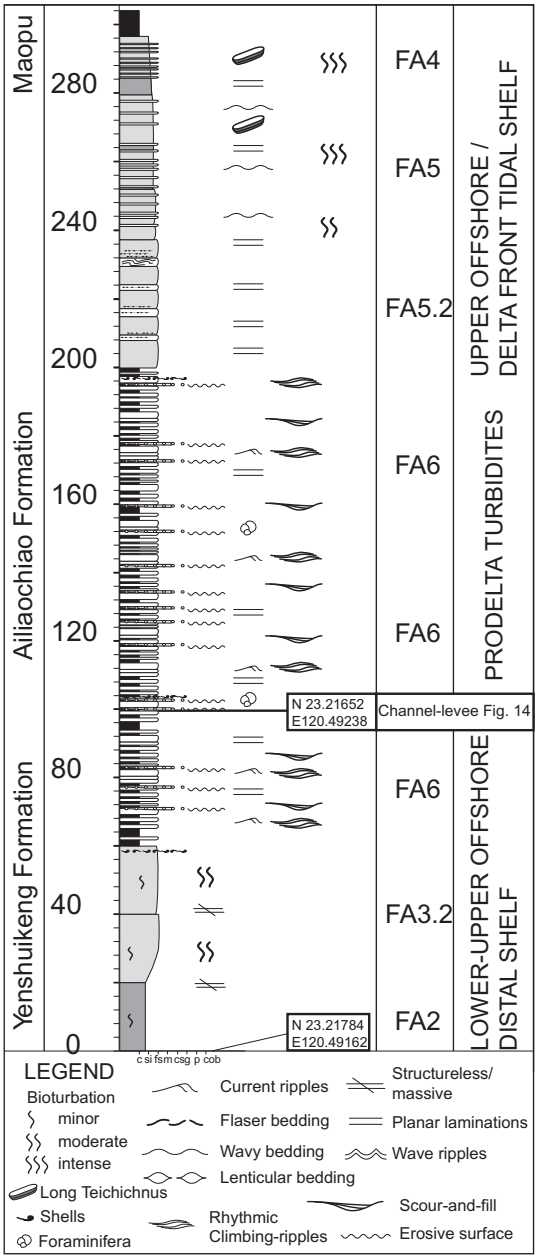

Fig. 5. Tseng Wen Toll, section (B), synthetic stratigraphic column (see Fig. 2 for location).

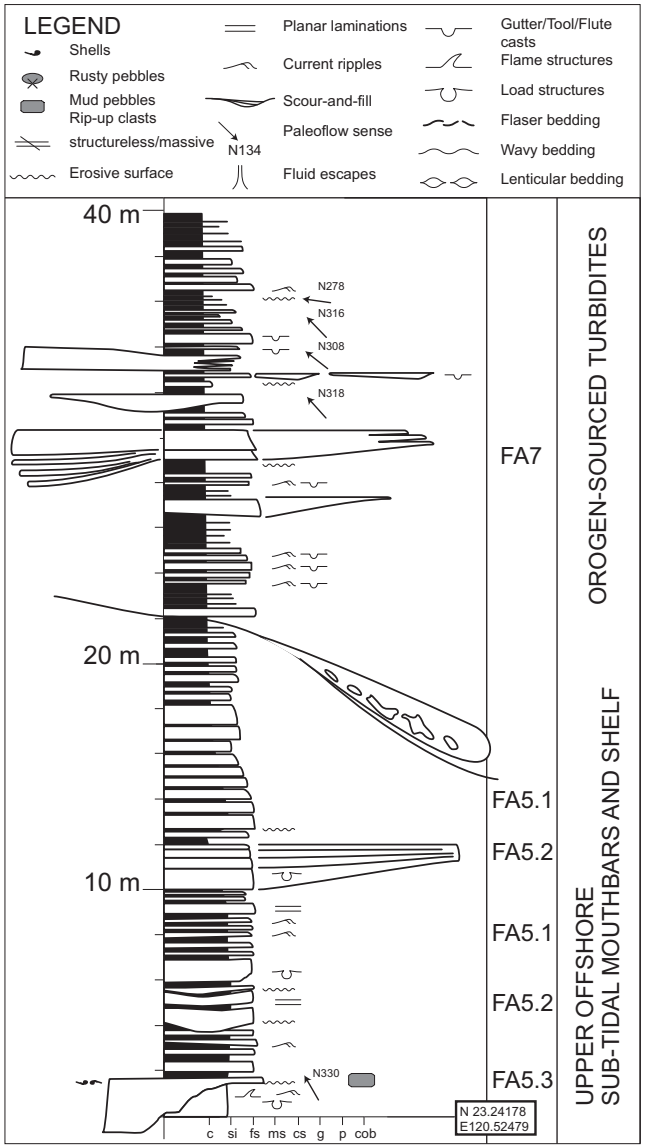

Fig. 6. Tseng Wen Dam, section (C), synthetic stratigraphic column (see Fig. 2 for location).

of probably tide-dominated deltas or estuaries of the large muddy Asian rivers draining the Chinese craton. Large areas of the shelf are covered by muddy or sandy sediments, their deposition is affected by oceanic currents, tides, storms and fluvial input to a varying degree. In the present case, the clastic material is brought in by the rivers to the shelf that are then reworked by waves and tides.

Consistent with this model is the observation in the Meishan and Tseng Wen Toll sections of marked small-scale repetitive alternation of both FA4.1 and FA4.2. In the Meishan section (Fig. 4), a 2 m long interval clearly exhibits this repetitive pattern (Fig. 9). The *Teichichnus* bioturbation systematically increases during sandier intervals immediately after the intervals of muddy lenticular and wavy ripple bedding. The sandy intervals after the bioturbation time are then often accompanied by coarser, tabular, less or not bioturbated decimetric sand beds of fine to medium grain size, sometimes associated with isolated decimetric scours and draping fill structures (Fig. 8 B). Since lamination very likely resulted from tides, these intervals formed in the order of less than a year and it can be proposed that the observed alternations of bioturbated sandy intervals and dark muddy intervals are the product of seasonal variations of the depositional environment.

An interesting analogue that could account for this observation exists currently in the Yellow Sea/east China Sea (Johnson and Baldwin, 1996) where seasonal reversal of oceanic and coastal currents combined with seasonal variation of storm intensity and fluvial input result in a similar sedimentation pattern; muddy zones related to cold southward currents are juxtaposed against sand zones formed by the warm northward flows. In this specific case, the northward flows corresponding to the summer monsoonal conditions are relatively gentle, accompanied by low sedimentation from suspension and allow a stratification of the water column and a high biogenic input from the surface. Thus the sandy bioturbated intervals represent summers. In contrast, the winters are characterized by severe storms that cause the resuspension of bottom sediment and the generation of turbid plumes with high sediment concentrations. Even though the increased action of storms is not directly observable in the studied section (Fig. 9) where we have instead attributed less energy to the muddier intervals, we believe

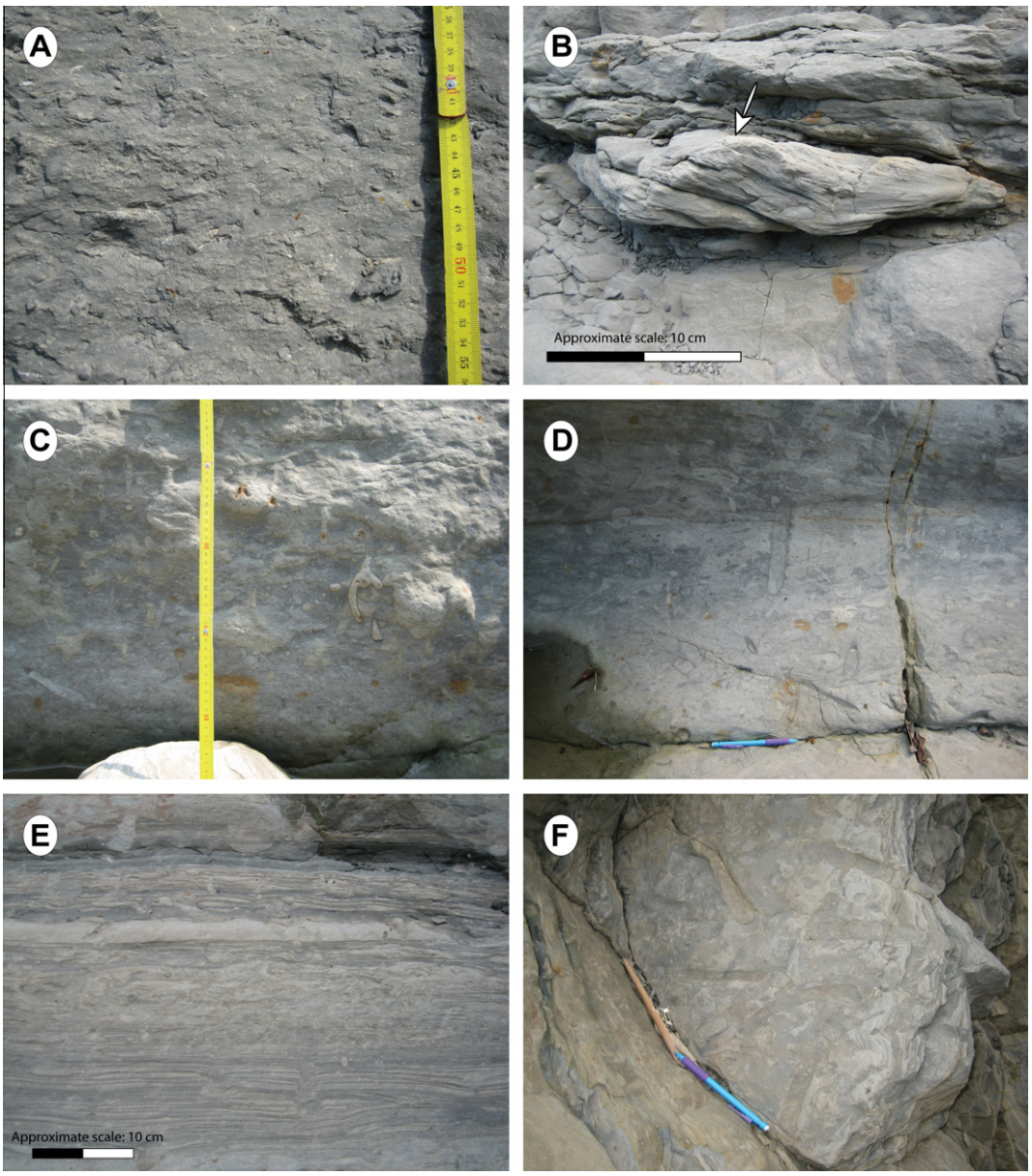

Fig. 7. Field photographs of facies from the Meishan section. (A) Close-view of the dark grey poorly sorted foraminiferal siltstones of FA2. Note the absence of physical structures, probably related to the intense biotubation (marked by shell concentrations in burrows). (B) Remnant flow structure preserved in fine sandstones of the FA3 assemblage. The incipient convex-upward form to the left of the structure (arrow) suggests possible hummocky cross-stratification bedform. (C) Example of trace fossils observable in the FA3, in this case *Thalassinoides*. (D) Different trace fossils assemblage in FA3. (E) Example of heterolithics of the FA4. The alternation between bioturbated and non-bioturbated periods is attributed to seasons. The internal lamination is interpreted to result from tidal currents on the shelf. (F) View from the top of a *Teichichnus* dominated interval of the FA4. Due to erosion the burrows can be observed in both horizontal and vertical section. Note the preferred orientation of the burrows, here about N20 (see arrow of the hand-held GPS).

that these intervals correspond to the winters. The possibly colder currents flowing southward at these periods may have been responsible for the migration or disappearance of the *Teichichnus* generating organisms. Perhaps, rather than salinity stress, the seasonal temperature variations associated with coastal and oceanic current reversals may have caused a yearly stress that could have caused the nearly monospecific *Teichichnus* dominance in these facies.

Such seasonal distribution changes of benthic populations are known to happen for example in the case of sea cucumbers (Holothurians, cf. Yamana et al., 2009), which would represent potential producers of *Teichichnus*.

A second observation worth noticing is the systematic alignment of the *Teichichnus* traces (Fig. 10). Several authors have previously noticed preferred orientation of elongate traces of for instance *Rhizocorralium* (Rodríguez-Tovar and Pérez-Valera, 2008) or *Diplocraterion* (Ekdale and Lewis, 1991; Fürsich, 1974). This is usually interpreted as a result of wave/tidal action control on the irrigation of burrows or on the current assisted food supply to the animals. Here, the *Teichichnus* burrows are oriented approximately parallel to the measured tidal currents in Meishan (~N045).

3.5. Facies Association 5: Wavy rhythmites and scoured sandstones: sub-tidal shelf and sand bodies (Fig. 8, occurrence: Meishan, Tseng Wen Toll and Dam)

3.5.1. Description

Five main facies compose this association: wavy rhythmites (FA5.1), sandstone (FA5.2) and conglomerate (FA5.3 and FA5.4) beds with scoured based, slumps and slides (FA5.5).

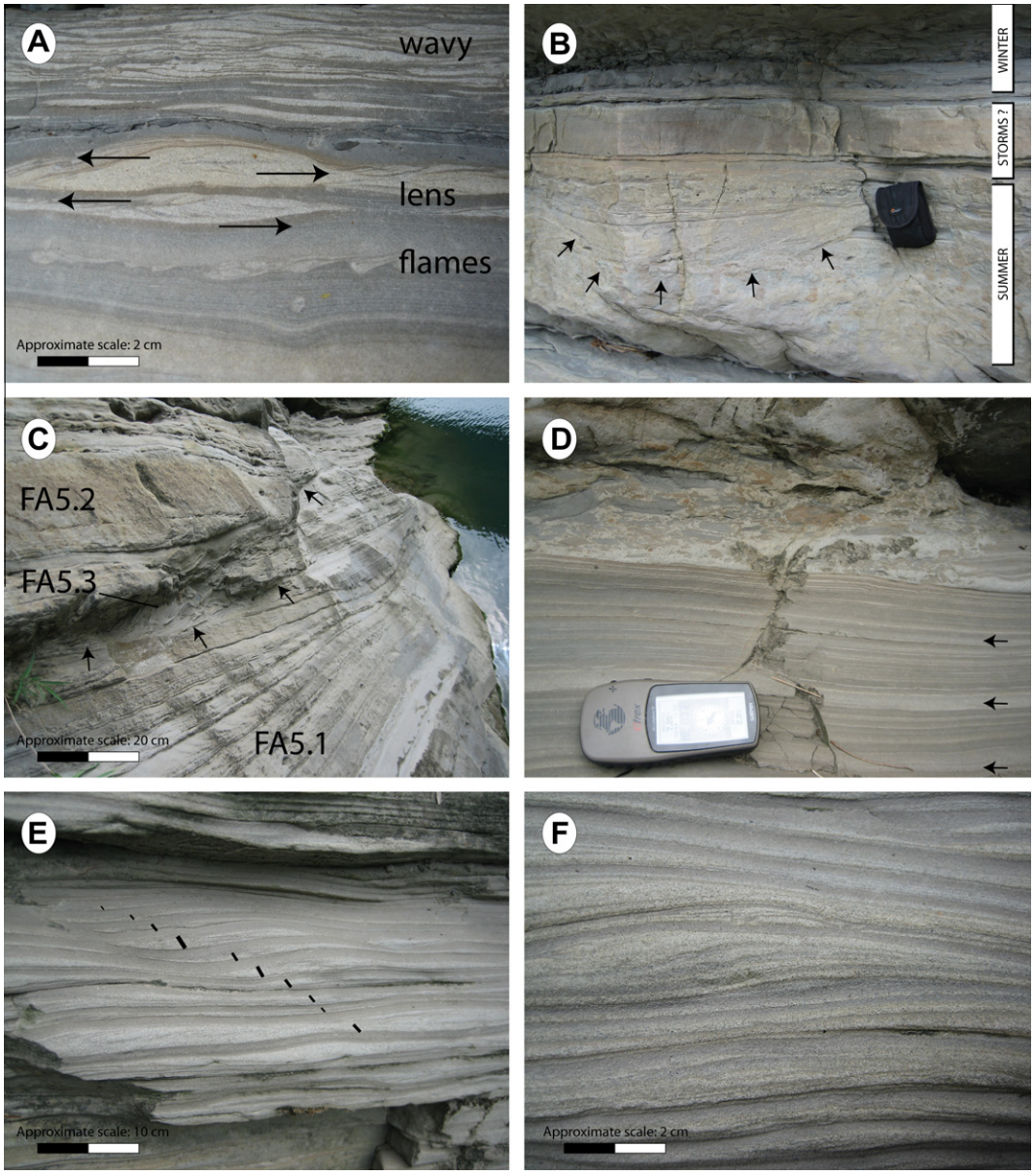

Fig. 8. Field photographs of facies from the Meishan section, continued. (A) Close-up view on lenticular bedding of the non-bioturbated facies of the FA4 assemblage. Current reversal attributed to tides can be observed within each lens, themselves separated by a fine-grained lamina (darker) probably corresponding to a slack stage. The very aggradational character of some of the lamination, as well as the concave-upward base of some of the rippled lenses could also suggest the influence of waves in building these bedforms. However, their systematically non-regular wave-length and amplitude, and the dominance of asymmetric forms suggests a dominance of current-related flows. Note the flame structures below. (B) Tabular sand bed and scour of the FA4. The large scour is visible in the centre left of the picture, underlined by arrows. The fine sand then fills in the scour, with less burrowing than in the preceding interval. The tabular sand bed, of fine to medium well sorted sands caps the whole. This type of succession can be attributed to the influence of storms, perhaps at the end of the summer (bioturbated interval) during the monsoon–typhoon periods. Camera case for scale is about 10 cm long. (C) Outcrop-scale view of assemblages FA5.1, FA5.2 and FA5.3. The wavy bedded rhythmites FA5.1 are eroded by a channel-size structure (small arrows). FA5.3 mud-rich conglomerates and then sand beds of FA5.2 fill in the scour. (D) Close-up view of thinly laminated rhythmites of FA5.1 and mud-rich conglomerate of FA5.3. Note the repetitive thinning–thickening of the sandier laminae in the rhythmites, indicated by the arrows. (E) View of the climbing-sigmoidal bedforms of the FA5.1 rhythmic facies. These forms are the product of several events as indicated by the succession of current-related coarser laminae and fall-out deposition related draping intervals of darker finer material. The draping intervals are of more even thickness. The coarser laminae systematically thicken in the lee side of the bedform. A noticeable feature is the thickening–thinning cyclic pattern in the sandy laminae (small dashes). These alternating sedimentation is attributed to tides and a relatively high proportion of suspension load in the sediment-laden flow. (F) Close-view of the sand-silt laminations in the FA5.1 facies.

3.5.1.1. FA5.1. Wavy bedded rhythmites. These are millimetric to pluricentimetric alternations of siltstones to fine sandstones with clayey–silty drapes (Fig. 8C–F). The bedding type is generally wavy, but flaser and lenticular bedding also occur. Two aspects are remarkable in these facies, the absence of bioturbation except some very rare horizontal *Protovirgularia* traces and a very strongly expressed rhythmic appearance constituted by coarse layers being regularly arranged between several millimetres to several centimetres thick muddy layers. This repetitive pattern also seems to display larger scale cycles of thinning and coarsening. The siltstones and sandstones layers generally show internal parallel lamination or asymmetric cross-lamination with mostly unimodal, but also bimodal current directions. These are always very small structures pointing to low current velocities. Some wave-like, bundled structures also occur. In many instances, the ripple trains have a decimetric–pluridecimetric wave-length and grow into

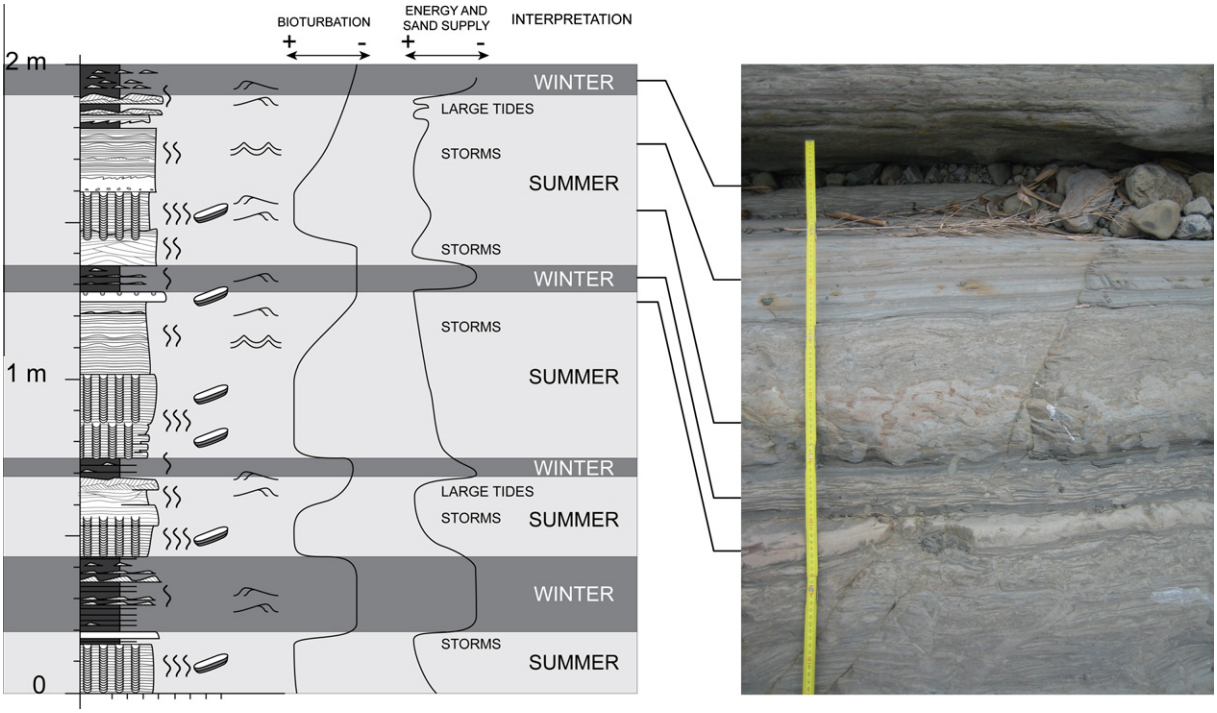

Fig. 9. Detailed sedimentological section and interpretation of regular alternations of burrowed and non-burrowed intervals of the FA4 assemblage. Because of the supposed tidal origin of the lamination, we estimate a yearly duration for the cycles that are a potential response to seasonal changes of environmental conditions. Such a record of seasonality in shallow-water sediments could be linked to early Asian monsoonal circulation patterns in the Pliocene.

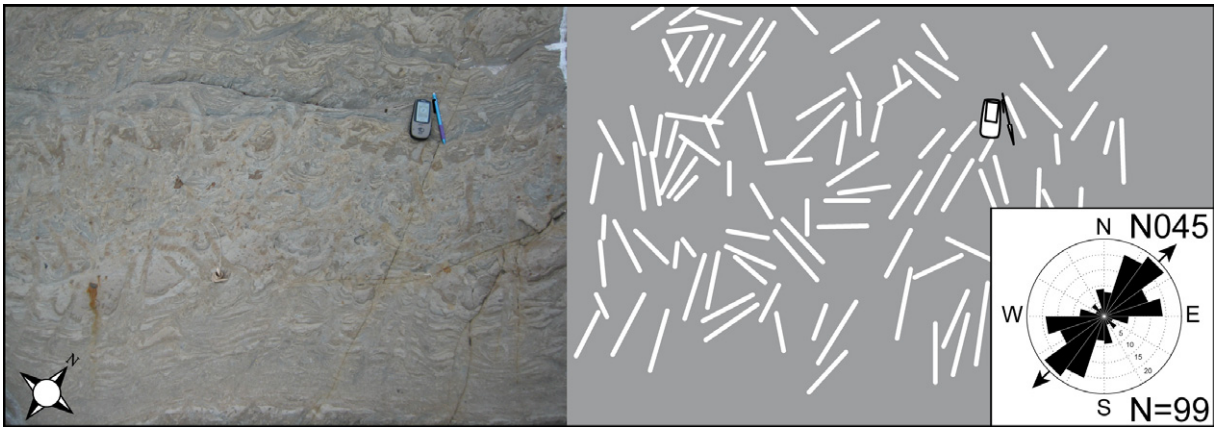

Fig. 10. Field photograph and simplified drawing of a bed surface seen from above with *Teichichnus* burrows. Most of the burrows are oriented to the N045 (note that the north of the rose diagram is to the north of the page, unlike the north of the picture). This alignment of traces results from directional hydrodynamics (waves, currents, tides) that probably affected the organisms' mechanical stability in their living environment, or the flow of food supply and the organisms orientation.

unidirectional climbing forms that sometimes become almost purely aggradational. A specific character of these climbing forms is that they keep the rhythmic character of alternating coarse–fine layers, showing that their migration–aggradation occurred as a discontinuous process of episodic current-related events separated by calm suspension fall-out periods.

3.5.1.2. FA5.2. Sand beds. Several centimetres to decimetres (30–40 cm) and metre thick beds of very fine to coarse sandstones with slightly to pronounced erosional bases overlay and interfinger with FA5.1 (Fig. 8 C).

Very fine to medium sandstones are generally thin and display a gentle or no grading and 3D and 2D current ripples at their tops. They contain small plant debris and laterally discontinuous patches of intraformational mud clasts (oxidized) conglomerates near the base. Some mud flakes and possible flaser bedding imply that the bulk of these beds could also be made of ripples but the homogeneous lithology prevents their observation. In some instances also large scale 3D megaripples (dunes) and cross-stratification are seen. The bed thickness varies over long wavelengths of ~10 m to several 10 s of metres; a bed may split-up laterally into two or more thinner beds that possibly grade into wavy bedded rhythmites of FA5.1. This implies lenticular sediment bodies some 100's of metres in size. No HCS and no wave ripples were observed in these beds. Burrows in the sandstones are generally rare to absent, some *Ophiomorpha* may occur.

Coarse sandstone beds are generally more erosive, with some examples showing clear large wave-length channel geometries. They can contain debris of shells (e.g. large oysters) and rip-up mud clasts. They are massive, with no grading, except the mud

clasts at the base. Laterally they sometimes grade directly into the wavy bedded rhythmites of FA5.1. The top of beds can display 3D sinuous ripples, but normally the massive beds do not show any flow related structures. Bioturbational structures were not observed in these beds.

3.5.1.3. FA5.3. Conglomerates. Two main types of conglomerates (Fig. 8C and D) occur in association with the above facies: mud-pebble conglomerates (FA5.3.1) and bioclastic conglomerates (FA5.3.2). The FA5.3.1 conglomerates form several decimetres to metre thick beds that have a very fine to coarse sandy matrix supporting rip-up clasts of initially soft material composed of FA5.1 rhythmic silts or undistinguishable muddy material supposedly originating from the fine-grained components of FA1 to FA4. These clasts are angular and several centimetres in size pointing to a short-range transport of cohesive sediment. Some rare shell debris of oysters were found towards the top of beds. The base of the FA5.3.1 conglomerates is slightly erosive, but no large channelized structures have been observed.

The FA5.3.2 are strongly cemented decimetric to metric conglomerate beds of centimetric to decimetric rip-up clasts similar to the clasts composing FA5.3.1, clasts of sandstones, and relatively large amounts of shell debris of, for instance, lamellibranchs (thick oysters) and gastropods. Some clasts of rhythmites and mud can reach a block size (several decimetres). Short borings may occur at the surface of sandstone cobbles.

3.5.1.4. FA5.4. Slumps. The sandstone beds and wavy rhythmites are in some instances (Meishan section) slumped and deformed. Internal deformation is marked by folding, faulting and numerous load and fluid escape structures, in particular in the sandstones. The absence of multiple refoldings, of largely scoured bases and of breccias and intraformational conglomerates in these facies indicates a small distance or very local soft deformation, and possibly relatively small sedimentary slopes. In addition, these facies are emplaced within the above described FA5.1 and FA5.2, which also suggests a local load induced slide.

3.5.2. Interpretation

The recurrent pattern of sand-mud couplets in FA5.1 has been studied in detail by measuring the thickness of each sand laminae within a 80 cm long section displaying particularly well expressed rhythmicities (Fig. 11). The measurements were done on digital pictures taken at a regular distance from the outcrop. This method allowed us to focus in and measure accurately sub-millimetric to millimetric laminations. A Fourier analysis to the thickness data of sand laminae shows a clear periodicity in the signal (Fig. 11 B and C) that is expressed in the frequency content by a peak at 33.3 laminae. This suggests deposition in a semi-diurnal or mixed tidal regime. While there are some clear 28 multiples (Fig. 13 B), the 33.3 dominant frequency instead of a pure 28 tides per neap-spring-neap cycle can be explained by the addition of random events due to storms or floods, for instance, and/or by perhaps lamina definition errors. Interpreting the exact regime of a tide-influenced depositional area is not always straightforward and should be made only through a thorough analysis of the observed cyclicities (De Boer et al., 1989; Mazumder and Arima, 2005). In the present study, the analysis simply confirms the tidal origin of the lamination.

This facies association is clearly marked by the influence of tides. The permanence of mud in the wavy rhythmites combined with the total absence of evidences of exposure suggests a subtidal environment. However, the lack of large scale tidal cross-stratification implies a relatively weak tidal regime and low current velocitites. Compared with the setting at the outlet of modern large Chinese rivers these sediments appear to be deposited in the distal part of extensive subaqueous deltas where they merge with the very low gradient muddy shelf. Currently, the sub-marine areas of the Taiwan Strait and of the Yellow Sea are covered by alternating large areas (>km^2) of sand and mud. Some of these sands are hectometric hydraulic bedforms (Boggs, 1974), whereas some are relict from summer currents (Johnson and Baldwin, 1996). Eventually, in the modern muddy deltas of the Yangtze and Huanghe, many slumps and slides occur on the delta-front (Bornhold et al., 1986; Lu et al., 1991; Prior et al., 1986b).

Therefore, the sub-marine landscape was composed of: (1) a muddy shelf merging with subaqueous deltas and constantly reworked by bottom tidal currents (FA5.1), (2) large-scale sand patches or sand bodies merging laterally with the muddy shelf and subaqueous delta-front (FA5.2 and FA5.3), and (3) a collapsing delta-front (FA5.4). As in the current setting, such a landscape can be relatively shallow (5–50 m) and with very low gradients (1°).

3.6. Facies association 6: Tseng Wen channel-levee system: pro-delta turbidites (Fig. 12, occurrence: Tseng Wen Toll)

3.6.1. Description

3.6.1.1. FA6.1. Laminated silts and sands. Centimetre to metre thick beds of siltstones to sandstones alternate with clayey–silty beds (Fig. 12A and B). The main feature is the fine-laminated character of fine (silt) to coarser (silt to medium) sand millimetric to centimetric alternations that form plane-parallel lamination, small current ripples or large climbing ripples with wavelength of 15–20 cm and amplitude of 1–2 cm. The large climbing ripples have climbing angles of usually 40–60° but sometimes being nearly vertical, resembling oscillation like, wavy aggrading ripples. In some cases, the ripples are contorted and deformed in current direction. At a smaller scale, small flame structures can be observed. The lamination, in particular within the climbing ripples, displays rhythmic thin–thick cycles very similar to those observed in the rhythmites of FA5.1. There is no significant thinning- or coarsening-upward trend in these beds. The base of beds are often erosive with scour-and-fill structures. Flute casts at the lower surface of scours have not been observed.

The few paleocurrent indicators point systematically to opposing directions to either side of the channel deposits (FA6.2, FA6.3; Fig. 13). In this case FA6.1 correspond to the distal end of the levees build by FA6.2 sand beds. Burrows are usually absent, only a few *Protovirgularia* and *Nereites missouriensis* may be present (Fig. 12 F).

3.6.1.2. FA6.2. Fine to coarse sand beds: lobe axis, proximal levee. The facies of FA6.1 grade laterally into decimetric to metric beds of sandstones of the FA6.2 (Fig. 12 C). These are poorly sorted quartz-dominated sands that also contain forams, small shell clasts, some large oyster clasts and intraformational mud and silts rip-up gravels and pebbles. The beds are fining-upward and have the largest clasts at the base and mainly sand towards the top. The often oxidized lithoclasts can give the exposed deposits a rusty appearance. The mud clasts are often washed away, marked by empty holes of pebble size. The primary sedimentary structures are low-angle lamination that are weakly expressed perhaps due to the rather uniform grain size. Both massive bedding and low-angle laminations grade laterally into dunes and climbing ripples of the FA6.1 assemblage. The bases of these beds are either non-erosive or form large-scale (metric, pluri-metric) channel-and-fill pattern (Fig. 12D and E). At smaller scale they do not show gutter, groove or flute casts on their surface. As mentioned above, in some cases, the sand beds of FA6.2 build on either sides of channels and merge laterally with FA6.1 climbing ripples bed accreting away from the channel axis (Fig. 13).

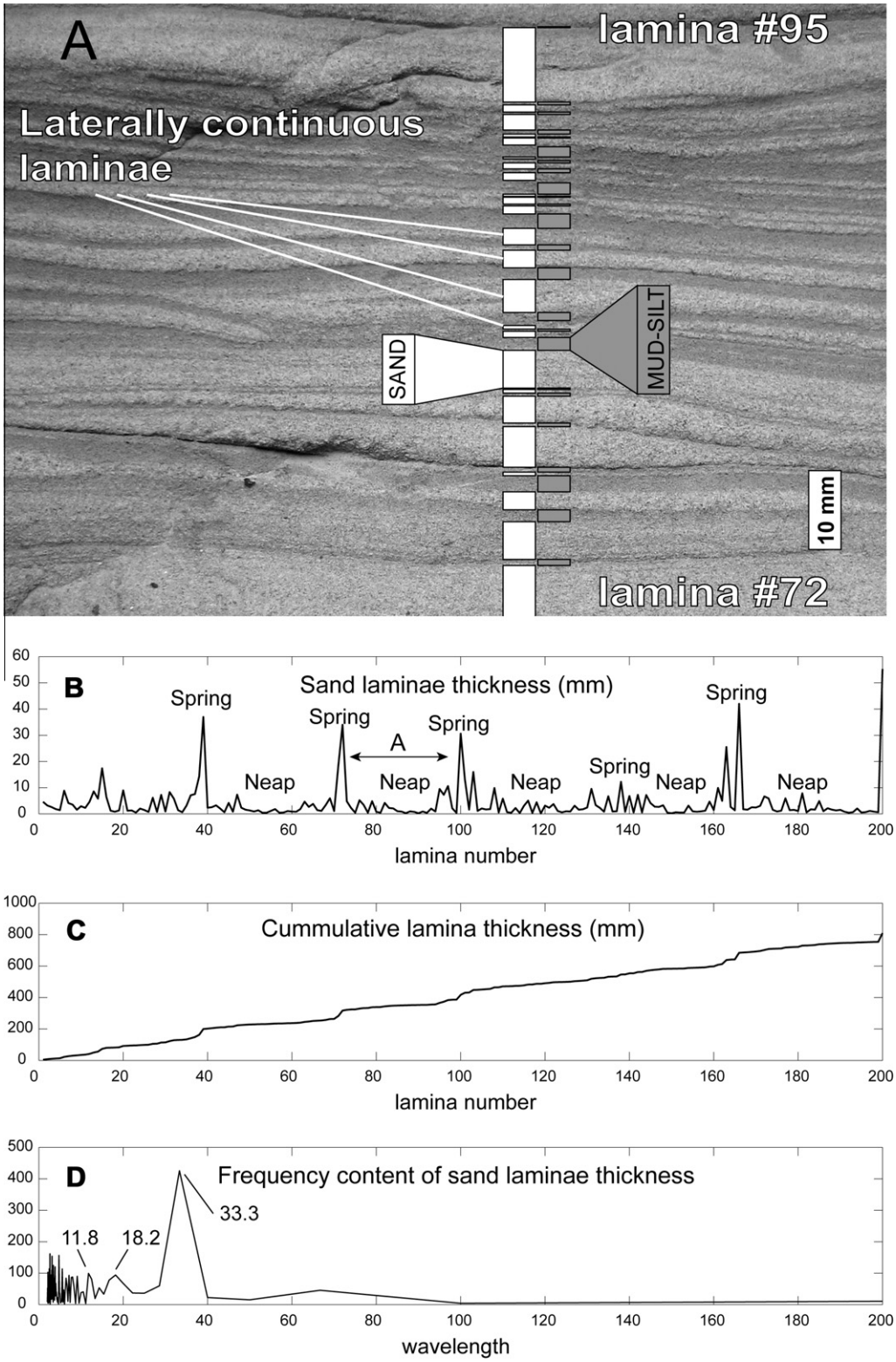

Fig. 11. Time series analysis of laminated wavy rhythmites of the FA5.1 assemblage. Two hundred sand laminae were measured over a 80 cm interval. We interpret the obtained 33.3 dominant signal as resulting from neap-spring cycles in a semi-diurnal tidal regime.

3.6.1.3. FA6.3. Conglomerates. These conglomerates are made-up of centimetric to pluri-decimetric silt- and sandstone clasts floating within a mud-dominated matrix (Fig. 12 D). The clasts are not sorted and their form is generally angular to sub-angular or rounded-folded when they are made of elements of FA6.1 or FA6.2. The beds are decimetre to several decimetres thick and occur as fill of channels and troughs having an erosive base. They are marked by abundant soft-sediment deformation structures such as folding and large-scale convolutes, giving an overall disturbed expression.

3.6.2. Interpretation

The general low fossil content, the absence of burrows, the alternating character imply periods of supply and periods of calm

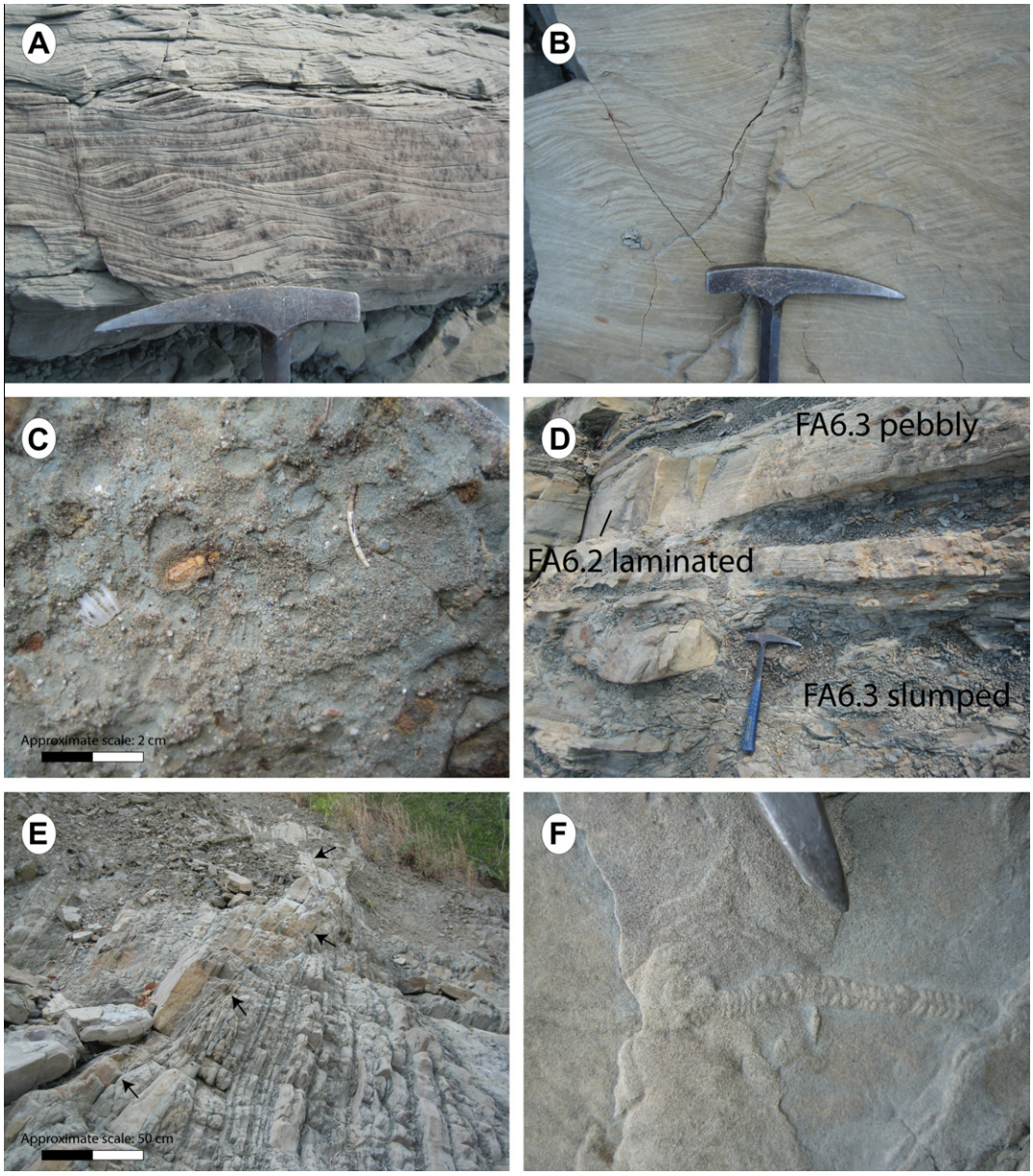

Fig. 12. Field photographs of facies from the Tseng Wen Channel-levee systems. (A and B) Sigmoidal climbing ripples in sub-marine pro-delta turbidite levee deposits (FA6.1). These ripples are asymmetric and climb with angles up to *ca.* 40° on photograph B. They are interpreted as resulting from unidirectional flows transporting silt and sand mostly in suspension. Because the finer grained laminae may represent periods of flow quiescence, these forms may be linked with the tidal currents acting on the shelf that dominate the other facies assemblages. (C) Close-up on the FA6.2 foraminiferal and bioclastic sandstones filling channel axis. (D) View of laminated sandstones, sandy matrix pebbly conglomerates and structureless conglomerates of slumped sandstones in a channel. (E) Example of the style and size (note the depth of the picture, such that the scale given is valid only for the foreground) of the large scours (arrows) that cut within the fine grained-distal levees. (F) Trace fossil *Protovirgularia* on a FA6.1 levee bed surface. The scarcity and low diversity of traces in these facies suggest their possible production by organisms exported from shallower environments during strong events. *Protovirgularia* is possibly associated with the displacement of Nuculoidean (bivalves) on the surface of the sandstone after its deposition. This suggest the episodic character of deposition ("event beds").

settling. The dominance of unidirectional currents and erosive surfaces suggests deposition in a fully marine environment affected by bottom currents in the form of suspension currents. Because of their association with shallow-marine sediments these deposits are interpreted as turbidites in a pro-delta environment or on the shelf. The observed channel-levee systems resemble high-density underflows and silt-flow gullies that can be observed on the slope of the modern Huanghe Delta (Prior et al., 1986a,b; Wiseman et al., 1986; Wright et al., 1986). The origin of these underflows can be related to river floods but the typical characteristics of hyperpycnites have not been observed (Mulder et al., 2003). As on the modern deltas of the Chinese coast, these sub-marine channels and flows can also be related to the redistribution of sediments sourced in slumps and slides of the delta-front (FA5.4 slumps and slides). However, the rhythmicity of the climbing ripples observed in the levees of channel systems exhibits strong similarities with the wavy rhythmites of FA5.1. Consequently, these pro-delta channel-levee systems could originate from slump events on the delta-front, and then be fed by the tidal bottom currents as also observed in the other outcrops or by a combination of tidal and river flood discharge events (Milliman et al., 1984).

Interestingly, Gibert and Domènech (2008) also observed *Protovirgularia* traces in turbiditic facies of shallow marine deposition in the Miocene of Catalunya, Spain. They could correspond to

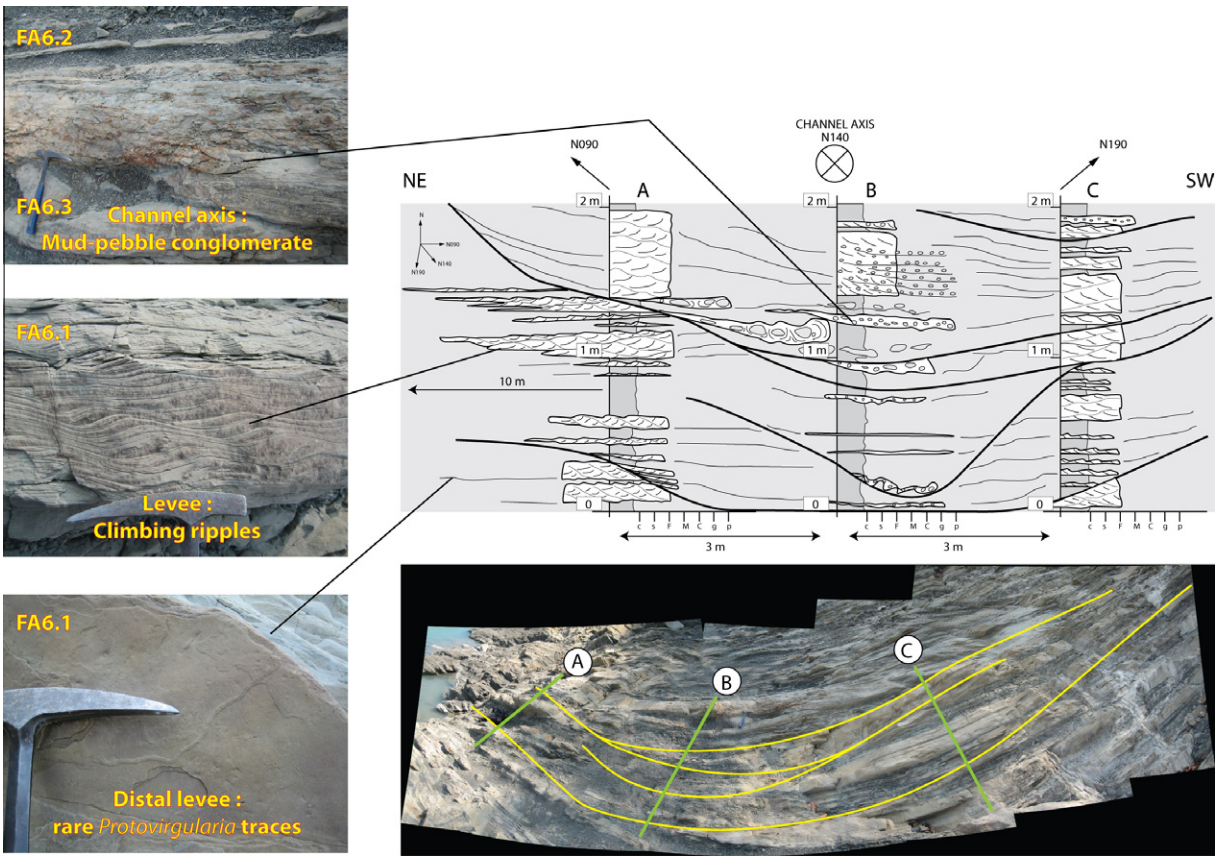

Fig. 13. Detailed description of a channel-levee system in Ailiaochiao pro-delta turbidites. Three detailed sections have been described and correlated at locations A, B and C as shown on the photographic panel. Pictures on the left show detailed illustrations of the different facies composing the channel-levee system. The flow azimuths are in opposite directions on either sides of the channel axis.

the locomotion traces of small bivalves, and their rarity suggests possible import from the shallow marine environments (Ekdale and Bromley, 2001; Wetzel et al., 2007) during erosive events.

3.7. Facies association 7: TsengWen Dam fine grained distal turbidites (Fig. 14, occurrence: Tseng Wen Dam)

3.7.1. Description

Typical are sand beds normally with erosive bases marked by flute casts (Fig. 14 C). The centimetres to decimetres thick beds are composed of quartz grains in silt to fine-sand size. The beds are normally graded and exhibit neither internal lamination nor parallel lamination, but some small-scale current ripples towards the base of the beds may occur. The thickness of the beds varies either as they fill in large-scale trough (Fig. 14 D) or as they pinch-out laterally forming large-scale (several metres wavelength) convex-upward sand bodies. The sand beds alternate with dark silts. Burrows have not been found in these deposits.

3.7.2. Interpretation

This facies association displays clear characteristics of turbidites. Because of the consistent paleo-flow azimuths to the west–northwest, we interpret them to be sourced to the east, from the growing orogen. They are significantly different from the FA6 channel-levee systems, which precludes a similar origin. An important aspect with respect to their depositional setting is their inclusion within a sedimentary succession of sub-tidal shelf facies of the FA5, and thus their shallow paleobathymetry.

4. Discussion

4.1. Paleoenvironments reconstruction (Fig. 15)

A model of paleoenvironments in Taiwan at the time of deposition of the Yutengping Sandstone/Ailiaochiao sandstones summarizes our observations (Fig. 15).

The fine grained facies associations FA1, FA2 and FA3 are found on a longitudinal proximal–distal profile perpendicular to the coastline. As energy decreases from the coast towards the centre of the basin, grain size decreases and bioturbation changes from *Cruziana* ichnofacies (FA3) to a distal unspecific totally bioturbated sediment (FA2) and lacking or hardly observed burrows in the most distal setting (FA1).

As explained above, the *Teichichnus* laminated silts and sands (FA4) mark specific conditions that can be attributed to either delta-front or shelf environments. In both cases we assign the laminated character of the sands to the influence of tides because of their well preserved rhythmicity and their association with other tide-dominated assemblages of the FA5. The nearly monospecific bioturbation can be attributed either to the influence of periodic freshwater influx into the deltaic environment or to rhythmic temperature and sediment transport variations associated with seasonal current reversals in the Taiwan Strait.

The wavy bedded rhythmites and scoured sandstones of FA5 correspond to tide-dominated delta-front environments. Paleo-flow directions usually indicate provenance from the Chinese margin. In the landscape reconstruction (Fig. 15) we assign these facies to several deltaic systems distributed along the Chinese margin paleo-shoreline supplying the basin from the west. Redistribution of

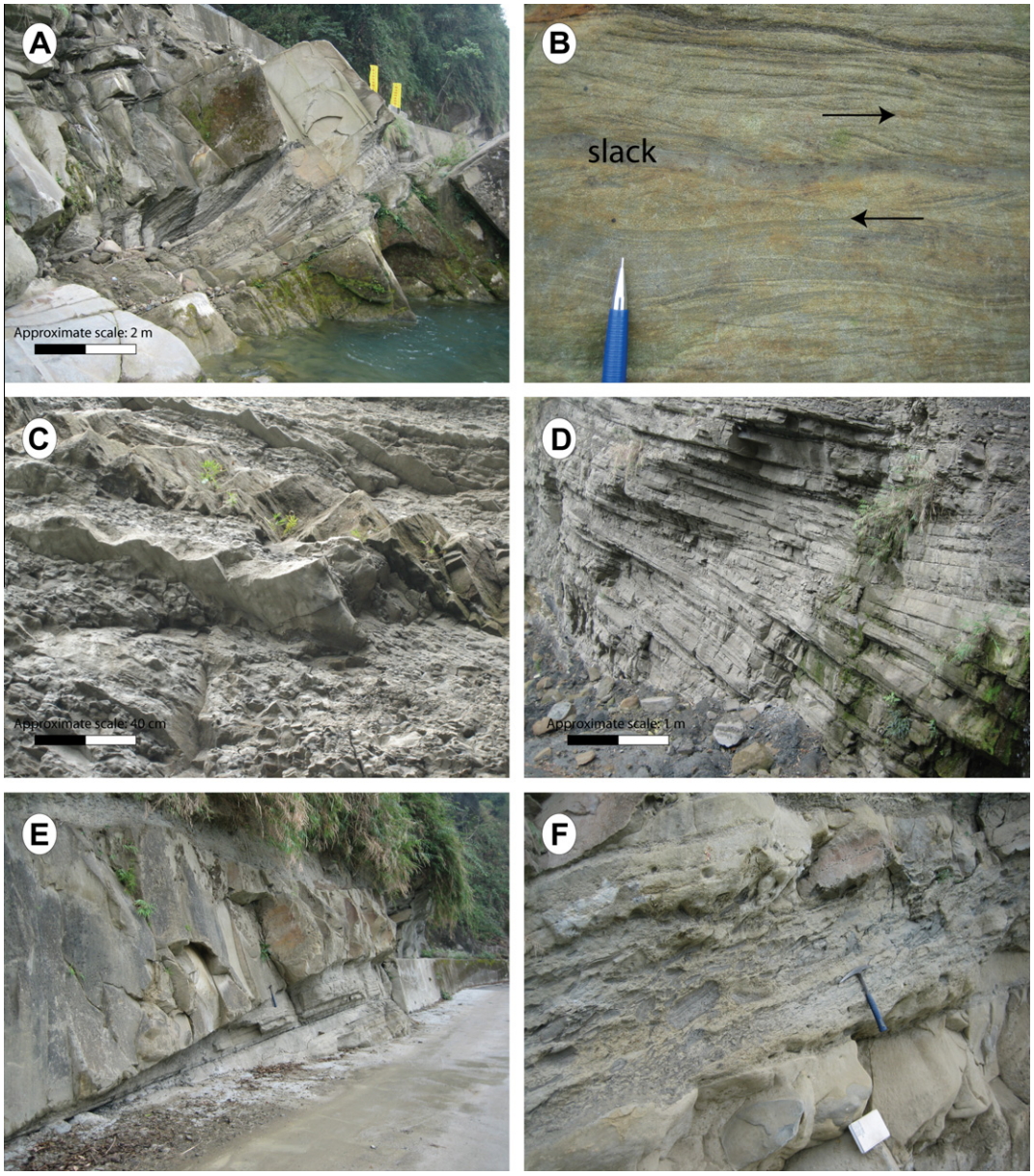

Fig. 14. Field photographs of the facies observed on the Tseng Wen Dam section. (A) Large-scale view of a sand body of FA5.2 grading laterally into rhythmites of the FA5.1 (below base of section C, Fig. 6). (B) FA5.1 rhythmites with current reversal (below base of section C, Fig. 6). (C) Erosive base of turbidite beds of FA7 with flute casts structures. (D) Laminated turbidite sand beds and lateral thickness variations. (E) FA5.2 sand body with erosive base into rhythmites of FA5.1 (the hammer is visible for scale in the centre of the photograph). (F) Mud-rich FA5.3 conglomerate on top of the channel sand body of photograph E.

some of this clastic input under the influence of tidal flows in the strait may have formed shelf sand bodies (Fig. 15).

The delta-front slumps and slides (FA5) as well as the channel-levee systems observed in pro-delta sediments (FA6) suggest that mass flow processes and possibly hyperpycnal sediment transport may have been important in this depositional environment. By analogy with the current setting offshore large Chinese rivers we attribute this character to the large supply of fine-grained material by rivers coming from the Chinese side of the strait. Trigger factors for mass flows and sea bed scouring could be related to slope instability of unconsolidated sediments under large accumulation rates but also to tidal and hyperpycnal currents and mass flows during large floods. The rhythmicity observed in some of the channel-levee sediments (FA6) suggests that sub-tidal currents could have also played an important role in sediment redistribution in these relatively distal systems.

It is possible that these channel-levee systems have initiated as slumps or slides and then became enhanced by hyperpycnal flood currents and sub-tidal flows.

Turbidite facies of the FA7 are integrated in this sedimentary landscape as "orogen-sourced" because of the observed paleo-flow directions to the north-east. However these are only local observations and of restricted areal extent. These turbidites could correspond to the northward equivalent of the lower Gutingkeng formation observed in the south of the Tainan basin.

The FA6 and FA7 assemblage of pro-delta and orogen-sourced turbidites are the deepest facies encountered in the present study. They provide a lower bound for the estimation of paleo-bathymetry. Analysis of benthic foraminifera in the lower Gutingkeng formation indicate an upper continental slope environment (Wang, 1992), and Covey (1986) proposed a depositional water depth of between 100 and 1000 m. However we note that coral reefs have

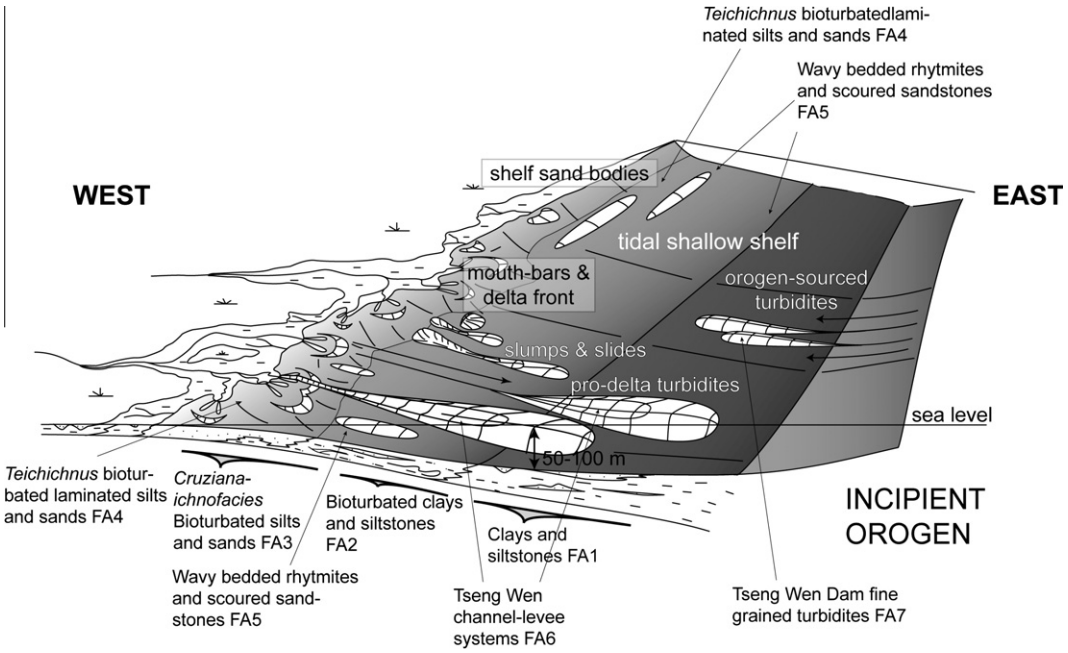

Fig. 15. Reconstructed depositional landscape during the Yutengping Sandstone and Ailiaochiao formations.

been observed on tectonic highs developed within this formation (Gong et al., 1998). It is unlikely in this high accumulation rate environments that highs of several hundred of metres of relief with respect to their surrounding basin have developed. In addition, the interfingering of the turbiditic facies with the pro-delta channel-levee systems suggests a low difference of depositional depth between the distal and the proximal deltaic environments. We propose that the deepest facies in the basin at the time of deposition of the Yutengping Sandstone, Ailiaochiao and lower Gutingkeng formation may not have exceeded a couple of hundred metres and perhaps have been closer to 50–100 m. The shallowest facies observed in our sections are the delta-front deposits of FA3 to FA5, deposited in 10–20 m water depth. No evidences of emergence have been found.

4.2. Margin physiography at the onset of collision (Fig. 16)

The physiography of the Chinese margin just prior to, or at the time of collision, is of importance to the study of the mechanism of mountain building in Taiwan.

The Yutengping/Ailiaochiao formations are interpreted to be deposited in the early stages of the collision when the mountains of Taiwan were just emerged. Their physiography must reflect strongly the physiography of the whole margin prior to, or at the time of, collision.

The map of Fig. 16 is a paleobathymetric reconstruction of the Chinese margin for the time of deposition of the Yutengping Sandstone/Ailiaochiao formations without representation of the nascent orogen and of sedimentary systems sourced in the east because their location and distribution remains too hypothetic based on our data. Existing paleobathymetric reconstructions at 6.5 Ma (e.g. Lin and Watts, 2002) show that western Taiwan and the Taiwan Strait represented a fluvial to shallow shelf setting prior to collision (e.g. Lin, 2001; Ting et al., 1991; Yu and Chow, 1997). It is known, and evident from our observations, that the Kueichulin formation indicates a transgression above the former margin deposits (e.g. Covey, 1984, 1986). The Yutengping sandstone and Ailiaochiao facies described in the present study show deeper environments than the facies preserved prior to 6.5 Ma. The shoreline was displaced to the west on the map of Fig. 16, until the limit of preservation of Kueichulin facies and equivalents on the center of the Penghu platform and the Kuanyin platform (Teng and Lin, 2004). The shoreline therefore follows closely the form of the basement contour (Lin and Watts, 2002).

According to balanced cross-sections by Mouthereau and Lacombe (2006), the series recorded in the Jioucyongping syncline of the Meishan area and in the Yuching syncline on the Tseng Wen river have encompassed respectively ~10 km and ~5 km of shortening in a N110° direction. The two stars on Fig. 16 indicate these two outcrops where delta-front and pro-delta turbidites have been restored in their original position.

Studies in the Hengchun Peninsula, i.e. the southern tip of Taiwan, show that it was in a slope setting (e.g. Sung and Wang, 1986) during deposition of the base of the Gutingkeng formation. Prior to collision the shelf break was in the vicinity of southern Taiwan, in a position very similar to its modern position. By unfolding the maximum eastward limit of the Kueichulin formation of ~28 km (total shortening, Mouthereau and Lacombe, 2006), a *minimum* position for the shelf break can be obtained since the Kueichulin formation is dominated by shelf facies. This shows that the shelf break location has remained in the vicinity of southern Taiwan during deposition of the Kueichulin formation. The reconstruction of the shelf break location (200 m isobath on Fig. 16) takes this into account and is consistent with reconstructions by Lin (2001), Lin and Watts (2002) and Teng (1990). Further south, the continent–ocean transition is preserved from collision and can still be observed today. Therefore, the position of the shelf-break south of the Taiwan Strait at the time of deposition of the Yutengping formation can be assumed as being the same as the modern.

This physiographic reconstruction highlights the largely non-cylindrical topography of the Chinese continental margin before and at the onset of collision. The Chinese continental margin eastern boundary probably drew a large westward protrusion, bulging the shelf break eastward, from the south of modern Taiwan to the north at the time of collision 6.5 Ma ago. This is also manifest on reconstructions by Lin (2001), Lin and Watts (2002), and Teng (1990).

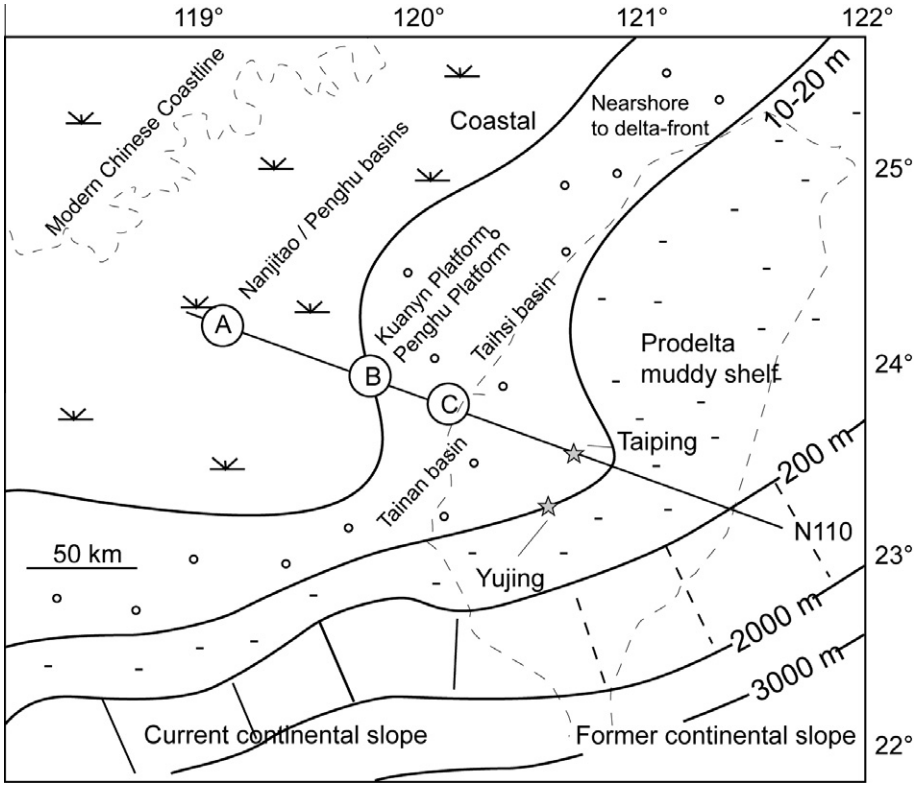

Fig. 16. Paleogeographic reconstruction of the west Taiwan basin showing inferred marine isobaths during deposition of the Yutengping Sandstone-Ailiaochiao formations, early Pliocene 4–5 Ma. Explanations in the text.

There is a fundamental distinction between this setting and the modern setting immediately south of Taiwan (Lin et al., 2008a,b) where collision is beginning, and further south where oceanic crust is still subducted. The modern Taiwan mountain range is situated mainly in place of this large promontory of the Chinese continental margin, and it is evident from the current geography that the collision is not happening progressively from north to south. In light of these considerations it can be suggested that the collision in Taiwan took place simultaneously along the length of the modern Taiwan mountains, approximately from the northern tip to somewhere close to the latitude of Kaohsiung in the south. The collision process is perhaps happening in a stepwise fashion from north to south as the Luzon Arc periodically hits the irregular Chinese margin.

It can be noted also that Covey's (1986) paleogeographic reconstructions already implied that the orogen developed almost at once when the Luzon Arc entered in collision with the Chinese margin and the Peikang high. However, Covey (1986) largely considered a progressive southward propagation in his model of foreland basin facies evolution, probably influenced by larger-scale kinematic model (Suppe, 1981).

According to this reconstruction and others in Tensi et al. (2006), the basin width at the time of the collision may have been of a maximum of 100 km. Considering that the collision occurred simultaneously along the length of the modern Taiwan mountains, the basin length could have been of a maximum of 300 km, and according to our paleobathymetric reconstructions, the basin water depth of no more than 200 m. This relatively large basin dimensions are probably responsible for the low amplitude of tides, compared with other narrower foredeeps (e.g. {Martel, 1994, #3234}).

4.3. Shallow marine turbidites in foreland basins

As explained in introduction, the foreland basin of Taiwan is one of the first basins where a "foreland sequence" with a underfilled to overfilled transition was identified. In his model, Covey (1986) proposed that the normal filling sequence of a foreland basin comprised an initial transgressive stage at the initation of foreland basin subsidence, in the present case the Kueichulin formation, a relatively deep water stage of under-fill when subsidence exceeds sediment input from the growing orogen (late Kueichulin, Chinshui Shale and Gutingkeng formations), and a third shallow water to fluvial stage of basin filling (Cholan) and over-filling (Toukoshan formation). This model was influenced by the north to south evolution of facies considered in parallel with the idea that the orogen had developed progressively southward (Suppe, 1981). Within this framework, the under-fill to over-fill model was also strongly influenced by considering that the current setting south of modern Taiwan corresponds to a early stage of the foreland basin fill, recognizing concurrently that the deepest facies encountered in the WFB were of comparatively shallow depositional depth.

This has led to a general model of foreland basin fill in which it is usually implied (Sinclair, 1997) that the under-fill deposition typically occurs at large water depth because of an imbalance between tectonic subsidence and sediment flux in favour of subsidence. Based on several foreland basin studies worldwide (e.g. Coakley and Watts, 1991; Graham et al., 1975; Grotzinger and McCormick, 1988; Houseknecht, 1986; Labaume and Séguret, 1985; Tankard, 1986), Sinclair (1997) formalized the underfilled trinity concept that was later successfully recognized in other foreland basins worldwide. Because of the intrinsic difficulty to quantify paleo-bathymetry of ancient deep sediments, it is however not

always clear how deep the basin generally was during the underfilled stage. Recently, Mutti et al. (2003, 2007) outlined the importance of recognizing shallow-water turbidites associated with river-fed deltas and hyperpycnal flows. According to Mutti et al. (2003, 2007), turbidite-like sandstone to mudstone beds of nearshore and shelfal environments are deposits commonly found in exposed fold-and-thrust belts basins (e.g. south-central Pyrenees, Spain; Neuquen Basin, Argentina; Tertiary Piedmont, northwestern Italy). These authors associate these deposits with dense hyperpycnal flows which produce facies tracts very similar to those of turbidites, except for the occurrence of hummocky cross-stratified sandstones, abundant bioturbation and fossil debris. Beyond these observations, the main criteria indicating the shallow-water depositional environment of these facies is their direct physical connection and interfingering with river-fed delta of which they are one element.

In the present case, it is manifest that the setting south of Taiwan is that of an accretionary wedge, with deep water sedimentation on oceanic crust, at the trench and on the wedge. As a difference, foreland basin deposition takes place on the continental crust and is bracketed in time by shelf deposition below and deltaic deposition above. It thus cannot be as deep as deposition happening currently in the south Taiwan accretionary wedge.

As in other basins worldwide (Sinclair, 1997) the foreland basin sequence in Taiwan is composed of shallow-water environments followed first by hemipelagics and then by turbiditic sandstones whose depositional depth depends upon the flexural response of the plate to the orogenic load (shallow turbidites in the case of Taiwan). There is no inherited bathymetry in the foreland and, therefore, the current setting south of modern Taiwan does not correspond to a early stage of the foreland basin fill.

4.4. Seasonality and the monsoon in the Pliocene

In the present study, observations have been presented of possible periodical facies evolution and migration of *Teichichnus* producing organisms (Fig. 11). Because of the tidal character of lamination observed in these facies this alternation between burrowed and non-burrowed facies is interpreted to be yearly and of seasonal origin.

This strong periodic character is not observed everywhere and is not necessarily general. It is facies-dependent and could simply mark the extreme sensitivity of a certain type of organism (producing the long *Teichichnus* burrows) to otherwise normal seasonal variations of one or several of the environmental parameters.

However, it is important to note that it may also be a record of increased seasonality and Monsoon in the Pliocene. Indeed, other authors have remarked on the seasonality of sediment supply to the Bengal shelf and fan during the Late Miocene (Davies et al., 2003).

The Taiwan Strait is affected by strong wind-driven oceanic currents, making it one of the most difficult zones for navigation in some periods of the year. Surface currents seem to be mainly directed to the north independently of the season (Chuang, 1986). But these may be stronger in the summer and weaker in the winter (Wu et al., 2007).

This contrasts with the activity of bottom currents (Johnson and Baldwin, 1996) which clearly shows seasonal reversal of currents and associated sedimentation zones. Cold southward currents in the winter leave turbid plumes and patches of mud which are juxtaposed with areas of sand deposition formed by the warm northward flows in the summers.

This situation might be complicated by the discharge of clastic material from the Chinese rivers strongly affected by the monsoonal variations of precipitation and erosion. For instance, the sediment and water discharge evolution at the mouth of the Yangtze river is clearly seasonal with a progressive increase from winter to summer, a strong peak in July, sometimes two peaks over the summer, and followed by a progressive return to winter conditions (Chen et al., 2001b).

These considerations lead to the interesting question as to whether the strong expression of seasonality recorded in Taiwan sedimentation may reveal the transformation of the Chinese shelf, opened eastwards to the ocean, into the Taiwan Strait bounded to the east by Taiwan mountains. This question highlights the need for further work in this direction, investigating the time of formation of the Taiwan Strait as a definite geographic entity.

5. Conclusion

In this work we have described and interpreted sedimentological observations on three detail sections of the Pliocene Yutengping/Ailiaochiao formations, deposited in the early stages of collision in Taiwan. Our results can be summarized as follows:

(1) We have found seven facies associations that record paleoenvironments of deposition ranging from nearshore to lower offshore with a strong influence of tidal reworking, probably even in the deeper sub-tidal environments, and facies recording mass flows in a pro-delta setting. In the studied series there is however no shallow facies demonstrating a particularly high tidal range such that the western basin of Taiwan in the early Pliocene may have already been similar to its current aspect, with a low tidal range but strong tidal influence on the shelf.

(2) The association of shallow facies of the upper offshore to lower shoreface with pro-delta turbidite facies sourced in the orogen in the east suggests a peculiar setting in which turbidite deposition occurred below wave base but on the shelf, in water depths of no more than 200 m and probably less (100 m). This adds to the examples of "shallow turbidites" increasingly commonly found in foreland basins (Mutti et al., 2007). The classical early "under-filled" stages of foreland basins must perhaps be not necessarily assumed "deep", as sometimes done. Basins such as the western Taiwan foreland basin develop on continental crust, when the accretionary prism in front of the "pro"-plate comes into contact with the ocean–continent transition and the associated shelf break, i.e. at relatively shallow depth.

(3) In some of the facies studied in this work we have found a possible seasonal signal in the form of rhythmic changes of sand-supply, water energy and bioturbation. This potentially suggests a marked seasonality affecting precipitation and sediment delivery as well as temperature. The Taiwan foreland basin may thus also present a potentially high-resolution record in shallow sediments of the early installation of monsoonal circulation patterns in east Asia.

(4) This sedimentological study allows us to confirm partly the paleogeography during the early stages of collision in Taiwan. The Chinese margin displayed a pronounced non-cylindrical geometry with a large basement promontory to the west in place of the modern Taiwan mountain range. This suggests that collision in Taiwan may have happened at once along the length of the current range, instead of progressively from north to south as sometimes envisaged.

Further analysis of these deposits in terms of petrography and sequence stratigraphy are still needed to better understand the complex plate interaction in this region (Kaus et al., 2009; Yamato et al., 2009).

Acknowledgments

This study was carried under funding of CNRS-INSU RELIEF project (PI Castelltort) and SNSF Swiss National Science Foundation Grant Number #200021-119841 to Castelltort and Kaus. We are pleased to thank Phillip Allen for his accurate review which improved the manuscript. We are indebted to Mr. Paul Chinen-Nan Yang and Tsun-You Pan for their assistance on the field. Rajat Mazumber is thanked for advising with the analysis of tidal series. And, we thank Slawek Jack and Olympia Giletycz for their invaluable help and welcome.

References

Allen, P.A., Homewood, P., Williams, G.D., 1986. Foreland basins: an introduction. In: Allen, P.A., Homewood, P. (Eds.), Foreland Basins. Spec. Publs Int. Ass. Sediment.. Blackwell Scientific Publications, pp. 3–12.

Barr, T.D., Dahlen, F.A., 1989. Brittle frictional mountain building 2. Thermal structure and heat budget. Journal of Geophysical Research 94 (B4), 3923–3947.

Boggs, S.J., 1974. Sand-wave fields in Taiwan Strait. Geology, 251–253.

Bornhold, B. et al., 1986. Sedimentary framework of the modern Huanghe (Yellow River) delta. Geo-Marine Letters 6 (2), 77–83.

Buatois, L.A., Santiago, N., Parra, K., Steel, R.J., 2008. Animal-substrate interactions in an Early Miocene wave-dominated tropical delta: delineating environmental stresses and depositional dynamics (Tácata Field, Eastern Venezuela). Journal of Sedimentary Research 78, 458–479.

Carmona, N.B., Buatois, L.A., Ponce, J.J., Mángano, M.G., 2009. Ichnology and sedimentology of a tide-influenced delta, Lower Miocene Chenque formation, Patagonia, Argentina: trace-fossil distribution and response to environmental stresses. Palaeogeography, Palaeoclimatology, Palaeoecology 273 (1–2), 75–86.

Chang, L.-S., 1955. Stratigraphy of Taiwan (in Chinese). Quarterly Journal Bank of Taiwan 36, 26–49.

Chang, S.S.L., Chi, W.-R., 1983. Neogene nannoplankton biostratigraphy in Taiwan and the tectonic implications. Petroleum Geology of Taiwan 19, 93–147.

Chemenda, A.I., Yang, R.K., Stephan, J.F., Konstantinovskaya, E.A., Ivanov, G.M., 2001. New results from physical modelling or arc-continent collision in Taiwan: evolutionary model. Tectonophysics 333 (1–2), 159–178.

Chen, C.-H. et al., 2000. Chiahsien, Sheet 51, Geological Map of Taiwan 1:50, 000. Central Geological Survey, MOEA.

Chen, W.S. et al., 2001a. Stratigraphic architecture, magnetostratigraphy, and incised-valley systems of the Pliocene–Pleistocene collisional marine foreland basin of Taiwan. Bulletin of the Geological Society of America 113 (10), 1249–1271.

Chen, Z., Li, J., Shen, H., Zhanghua, W., 2001b. Yangtze River of China: historical analysis of discharge variability and sediment flux. Geomorphology 41 (2–3), 77–91.

Chiang, C.S., Yu, H.S., Chou, Y.W., 2004. Characteristics of the wedge-top depozone of the southern Taiwan foreland basin system. Basin Research 16 (1), 65–78.

Chuang, W.-S., 1986. A note on the driving mechanisms of current in the Taiwan Strait. Journal of the Oceanographical Society of Japan 42, 355–361.

Coakley, B.J., Watts, A.B., 1991. Tectonic controls of the development of unconformities: the North Slope, Alaska. Tectonics 10 (1), 101–130.

Covey, M., 1984. Sedimentary and tectonic evolution of the western Taiwan foredeep. Princeton University, 152 p.

Covey, M., 1986. The evolution of foreland basins to steady state: evidence from the western Taiwan foreland basin. In: Allen, P.A., Homewood, P., (Eds.), Foreland Basins, vol. 8. Blackwell Scientific, Special Publication – International Association of Sedimentologists, pp. 77–90.

Dadson, S.J. et al., 2003. Links between erosion, runoff variability and seismicity in the Taiwan Orogen. Nature (London) 426 (6967), 648–651.

Dahlen, F.A., Barr, T.D., 1989. Brittle frictional mountain building 1. Deformation and mechanical energy budget. Journal of Geophysical Research 94 (B4), 3906–3922.

Davies, C., Best, J., Collier, R., 2003. Sedimentology of the Bengal shelf, Bangladesh: comparison of late Miocene sediments, Sitakund anticline, with the modern, tidally dominated shelf. Sedimentary Geology 155 (3–4), 271–300.

De Boer, P.L., Oost, A.P., Visser, M.J., 1989. The diurnal inequality of the tide as a parameter for recognizing tidal influences. Journal of Sedimentary Research 59 (6), 912–921.

Ekdale, A.A., Bromley, R.G., 2001. A day and a night in the life of a cleft-foot clam: *Protovirgularia*–Lockeia–Lophoctenium. Lethaia 34 (2), 119–124.

Ekdale, A.A., Lewis, D.W., 1991. Trace fossils and paleoenvironmental control of ichnofacies in a late Quaternary gravel and loess fan delta complex, New Zealand. Palaeogeography, Palaeoclimatology, Palaeoecology 81, 253–279.

Ernst, W.G., Jahn, B.M., 1987. Crustal accretion and metamorphism in taiwan, a post-palaeozoic mobile belt. Philosophical Transactions of the Royal Society of London. Series A, Mathematical and Physical Sciences 321 (1557), 129–161.

Fuller, C.W., Willett, S.D., Fisher, D., Lu, C.Y., 2006. A thermomechanical wedge model of Taiwan constrained by fission-track thermochronometry. Tectonophysics 425 (1–4), 1–24.

Fürsich, F.T., 1974. On *Diplocraterion* Torrel 1870 and the significance of morphological features in vertical spreiten-bearing, U-shaped trace fossils. Journal of Paleontology 48, 952–962.

Gibert, J.M.D., Domènech, R., 2008. Trazas fósiles de nuculoideos (*Protovirgularia*) del Mioceno marino de la cuenca del Vallès-Penedès. Revista Española de Paleontología 23 (2), 129–138.

Gong, S.-Y., Wang, S.-W., Lee, T.-Y., 1998. Pleistocene coral reefs associated with claystones, Southwestern Taiwan. Coral Reefs 17, 215–222.

Graham, S.A., Dickinson, W.R., Ingersoll, R.V., 1975. Himalayan-Bengal model for flysch dispersal in the Appalachian-Ouachita system. GSA Bulletin 86, 273–286.

Grotzinger, J.P., McCormick, D.S., 1988. Flexure of the Early Proterozoic lithosphere and the evolution of the Kilohigok basin (1.9 Ga), northwest Canadian Shield. In: Kleinspehn, K., Paola, C. (Eds.), New Perspectives in Basin Analysis. Springer-Verlag, New York, pp. 405–430.

Ho, C.S., 1986. A synthesis of the geologic evolution of Taiwan. Tectonophysics 125 (1–3), 1–16.

Ho, C.S. (Ed.), 1988. An introduction to the geology of Taiwan: explanatory text of the geological map of Taiwan. Central Geological Survey, The Ministry of Economic Affairs, Taiwan, Republic of China.

Horng, C.S., Shea, K.S., 1996. Dating of the Plio-Pleistocene rapidly deposited sequence based on integrated magneto-biostratigraphy: a case study of the Madagida-chi Section, Coastal Range, eastern Taiwan. Journal of the Geological Society of China 39 (1), 31–58.

Houseknecht, D.W., 1986. Evolution from passive margin to foreland basin: the Atoka formation of the Arkoma Basin, south-central USA. In: Allen, P.A., Homewood, P., (Eds.), Foreland Basins, vol. 8. Blackwell Scientific, Special Publication – International Association of Sedimentologists, pp. 327–345.

Huang, T.C., 1984. Planktonic foraminiferal biostratigraphy and datum planes in the neogene sedimentary sequences in Taiwan. Palaeogeography, Palaeoclimatology, Palaeoecology 46, 97–106.

Johnson, H.D., Baldwin, C.T., 1996. Shallow clastic seas. In: Reading, H.G. (Ed.), Sedimentary Environments: Processes. Facies and Stratigraphy. Blackwell Publishing, pp, pp. 232–280.

Juang, W.-S., 1996. Geochronology and geochemistry of basalts in the Western Foothills, Taiwan. Bulletin National Museum of Natural Sciences 7, 45–98.

Kaus, B.J.P., Liu, Y., Becker, T.W., Yuen, D.A., Shi, Y., 2009. Lithospheric stress-states predicted from long-term tectonic models: influence of rheology and possible application to Taiwan. Journal of Asian Earth Sciences 36 (1), 119–134.

Labaume, P., Séguret, M., 1985. Evolution of a turbiditic foreland basin and analogy with an accretionary prism: exemple of the Eocene south-Pyrenean basin. Tectonics 4 (7), 661–685.

Lin, C.-C. (Ed.), 1954. Geology of Taiwan (in Chinese). China Publishing Foundation, Taipei, Taiwan.

Lin, A.T., 2001. Cenozoic stratigraphy and tectonic development of the West Taiwan Basin. PhD Thesis, Oxford University.

Lin, A.T., Watts, A.B., 2002. Origin of the West Taiwan basin by orogenic loading and flexure of a rifted continental margin. Journal of Geophysical Research B: Solid Earth 107 (9), 1–2.

Lin, A.T., Watts, A.B., Hesselbo, S.P., 2003. Cenozoic stratigraphy and subsidence history of the South China Sea margin in the Taiwan region. Basin Research 15 (4), 453–478.

Lin, C.-C. et al., 2004. Yunlin, Sheet 38, Geological Map of Taiwan, 1:50, 000. Central Geological Survey, MOEA.

Lin, C.-C. et al., 2005. Sinhua, Sheet 50, Geological Map of Taiwan, 1:50, 000. Central Geological Survey, MOEA.

Lin, A.T. et al., 2008a. Tectonic features associated with the overriding of an accretionary wedge on top of a rifted continental margin: an example from Taiwan. Marine Geology 255 (3–4), 186–203.

Lin, A.T., Yao, B., Hsu, S.K., Liu, C.S., Huang, C.Y., 2008b. Tectonic features of the incipient arc-continent collision zone of Taiwan: implications for seismicity. Tectonophysics 479, 28–42.

Liu, T.K., Hsieh, S., Chen, Y.G., Chen, W.S., 2001. Thermo-kinematic evolution of the Taiwan oblique-collision mountain belt as revealed by zircon fission track dating. Earth and Planetary Science Letters 186 (1), 45–56.

Lu, N. et al., 1991. Sediment thixotropy and submarine mass movement, Huanghe Delta, China. Geo-Marine Letters 11 (1), 9–15.

Mazumder, R., Arima, M., 2005. Tidal rhythmites and their implications. Earth-Science Reviews 69, 79–95.

Martel, A.T., Allen, P.A., Slingerland, R., 1994. Use of tidal-circulation modeling in paleogeographical studies: an example from the Tertiary of the Alpine perimeter. Geology 22 (10), 925–928.

Milliman, J.D. et al., 1984. Tidal phase control of sediment discharge from the Yangtze River. Estuarine, Coastal and Shelf Science 19, 119–128.

Mouthereau, F., Lacombe, O., 2006. Inversion of the Paleogene Chinese continental margin and thick-skinned deformation in the Western Foreland of Taiwan. Journal of Structural Geology 28 (11), 1977–1993.

Mulder, T., Syvitski, J.P.M., Migeon, S., Faugères, J.-C., Savoye, B., 2003. Marine hyperpycnal flows: initiation, behavior and related deposits. A review. Marine and Petroleum Geology 20 (6–8), 861–882.

Mutti, E., Tinterri, R., Benevelli, G., Biase, D.d., Cavanna, G., 2003. Deltaic, mixed and turbidite sedimentation of ancient foreland basins. Marine and Petroleum Geology 20 (6–8), 733–755.

Mutti, E., Tinterri, R., Magalhaes, P.M., Basta, G., 2007. Deep-water turbidites and their equally important shallow-water cousins. Search and Discovery.

Pemberton, S.G., et al. (Eds.), 2001. Ichnology and Sedimentology of Shallow to Marginal Marine Systems. Short Course Notes, 15. Geological Association of Canada, St. John's, Newfoundland, Canada.
Prior, D. et al., 1986a. The subaqueous delta of the modern Huanghe (Yellow River). Geo-Marine Letters 6 (2), 67–75.
Prior, D. et al., 1986b. Active slope failure, sediment collapse, and silt flows on the modern subaqueous Huanghe (Yellow River) delta. Geo-Marine Letters 6 (2), 85–95.
Rodríguez-Tovar, F.J., Pérez-Valera, F., 2008. Trace fossil *Rhizocorallium* from the Middle Triassic of the Betic Cordillera, Southern Spain: characterization and environmental implications. Palaios 23, 78–86.
Seno, T., Stein, S., Gripp, A.E., 1993. A model for the motion of the Philippine Sea Plate consistent with NUVEL-1 and geological data. Journal of Geophysical Research 98(B10).
Shaw, C.L., 1996. Stratigraphic correlations and isopach maps of the western Taiwan Basin. Terrestrial, Atmospheric and Oceanic Sciences 7, 333–360.
Sibuet, J.C., Hsu, S.K., 1997. Geodynamics of the Taiwan arc–arc collision. Tectonophysics 274 (1–3), 221–251.
Simoes, M., Avouac, J.P., 2006. Investigation the kinematics of mountain building in Taiwan from the spatiotemporal evolution of the foreland basin and western foothills. Journal of Geophysical Research B: Solid Earth 111 (10).
Sinclair, H.D., 1997. Tectonostratigraphic model for underfilled peripheral foreland basins: an Alpine perspective. Bulletin of the Geological Society of America 109 (3), 324–346.
Sung, Q., Wang, Y., 1986. Sedimentary environments of the Miocene sediments in the Hengchun Peninsula and their tectonic implications. Memoir of the Geological Society of China 7, 325–340.
Suppe, J., 1980. A retrodeformable cross section of northern Taiwan. Proceedings Geological Society of China 23, 46–55.
Suppe, J., 1981. Mechanics of mountain building and metamorphism in Taiwan. Memoir of the Geological Society of China (Taiwan) 4, 67–89.
Suppe, J., 1984. Kinematics of arc-continental collision, flipping of subduction, and back-arc spreading near Taiwan. Memoir of the Geological Society of China (Taiwan) 6, 21–33.
Tankard, A.J., 1986. On the depositional response to thrusting and lithospheric flexure: examples from the Appalachian and Rocky Mountain basins. In: Allen, P.A., Homewood, P., (Eds.), Foreland Basins, vol. 8. Blackwell Scientific, Special Publication – International Association of Sedimentologists, pp. 369–392.
Teng, L.S., 1990. Geotectonic evolution of late Cenozoic arc-continent collision in Taiwan. Tectonophysics 183 (1–4), 57–76.
Teng, L.S., 1991. Tectonic aspects of the Paleogene depositional basin of northern Taiwan. Proceedings – Geological Society of China 34 (4), 313–335.
Teng, L.S., 1996. Extensional collapse of the northern Taiwan mountain belt. Geology 24 (10), 949–952.
Teng, L.S., Lin, A.T., 2004. Cenozoic tectonics of the China continental margin: Insights from Taiwan. In: Malpas, J., Fletcher, C.J., Aitchinson, J.C., Ali, J. (Eds.), Aspects of the Tectonic Evolution of China, vol. 226. Special Publications, Geological Society of London, London, pp. 313–332.
Tensi, J., Mouthereau, F., Lacombe, O., 2006. Lithospheric bulge in the West Taiwan Basin. Basin Research 18 (3), 277–299.
Ting, H.-H., Huang, C.-Y., Wu, L.-C., 1991. Paleoenvironments of the late Neogene sequences along the Nantzuhsien River, southern Taiwan. Petroleum Geology of Taiwan 26, 121–149.
Tsai, Y.-B., 1986. Seismotectonics of Taiwan. Tectonophysics 125, 17–37.
Wang, C.M., 1992. Paleoecology of the Pleistocene benthic foraminifers of the Chisan section, southwestern Taiwan. MSc Thesis. National Taiwan University, Taipei (in Chinese).
Wetzel, A., Blechschmidt, I., Uchman, A., Matter, A., 2007. A highly diverse ichnofauna in Late Triassic deep-sea fan deposits of Oman. PALAIOS 22 (5), 567–576.
Wiseman, W. et al., 1986. Suspended sediment advection by tidal currents off the Huanghe (Yellow River) delta. Geo-Marine Letters 6 (2), 107–113.
Wright, L. et al., 1986. Hyperpycnal plumes and plume fronts over the Huanghe (Yellow River) delta front. Geo-Marine Letters 6 (2), 97–105.
Wu, F.T., Rau, R.J., Salzberg, D., 1997. Taiwan orogeny: thin-skinned or lithospheric collision? Tectonophysics 274 (1–3), 191–220.
Wu, C.-R., Chao, S.-Y., Hsu, C., 2007. Transient, seasonal and interannual variability of the Taiwan Strait current. Journal of Oceanography 63, 821–833.
Yamana, Y., Hamano, T., Goshima, S., 2009. Seasonal distribution pattern of adult sea cucumber Apostichopus japonicus (Stichopodidae) in Yoshimi Bay, western Yamaguchi Prefecture, Japan. Fisheries Science 75 (3), 585–591.
Yamato, P., Mouthereau, F., Burov, E., 2009. Taiwan mountain building: Insights from 2-D thermomechanical modelling of a rheologically stratified lithosphere. Geophysical Journal International 176 (1), 307–326.
Yu, H.S., Chou, Y.W., 2001. Characteristics and development of the flexural forebulge and basal unconformity of Western Taiwan Foreland Basin. Tectonophysics 333 (1–2), 277–291.
Yu, H.S., Chow, J., 1997. Cenozoic basins in northern Taiwan and tectonic implications for the development of the eastern Asian continental margin. Palaeogeography, Palaeoclimatology, Palaeoecology 131 (1–2), 133–144.
Yu, S.B., Chen, H.Y., Kuo, L.C., 1997. Velocity field of GPS stations in the Taiwan area. Tectonophysics 274 (1–3), 41–59.